THE HIGH ENERGY SOLAR SPECTROSCOPIC IMAGER

SMALL-CLASS EXPLORER PROPOSAL IN RESPONSE TO NASA AO-97-OSS-03

JUNE 1997

HESSI

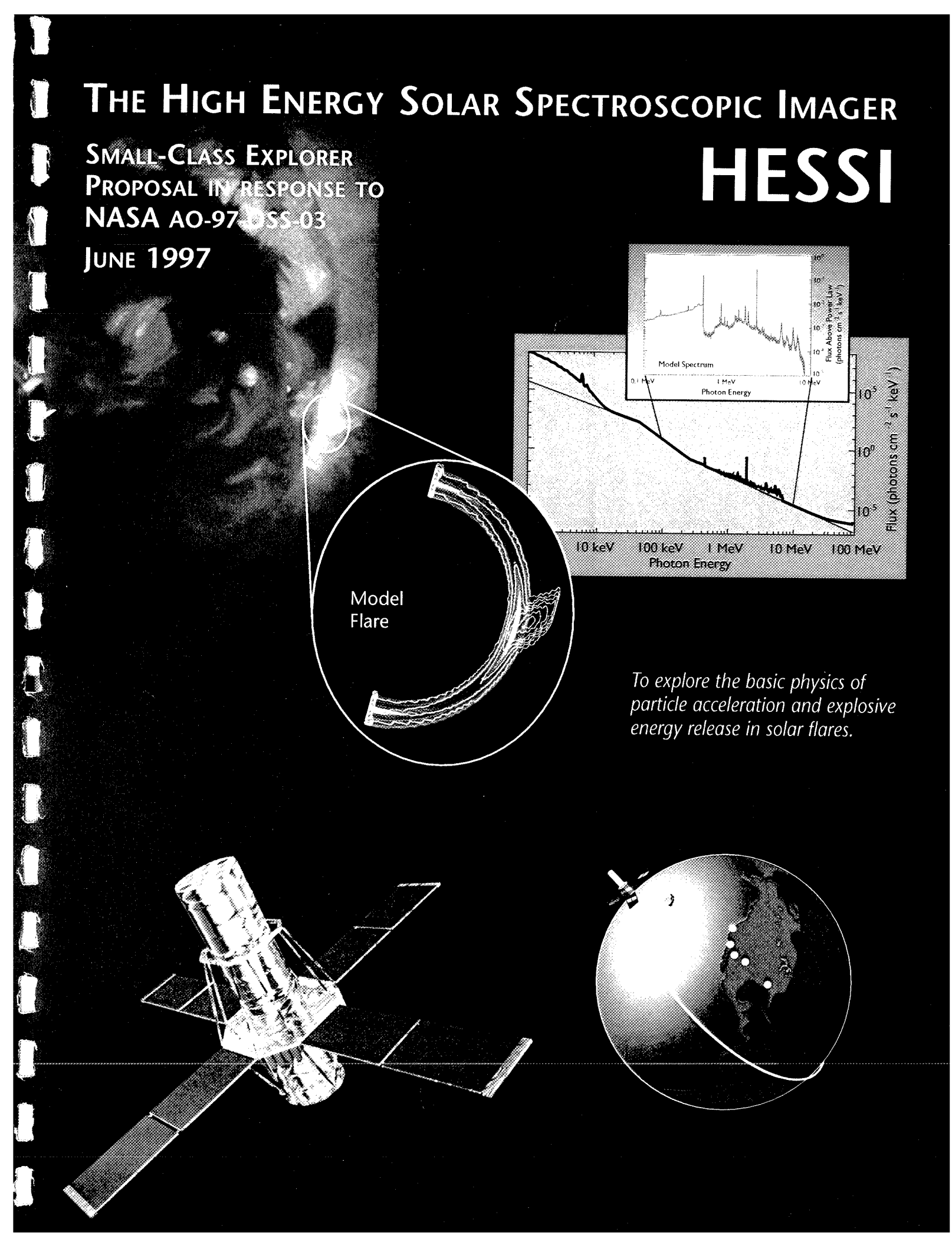

To explore the basic physics of particle acceleration and explosive energy release in solar flares.

A. INVESTIGATION SUMMARY

Small Explorer and Missions of Opportunity
Investigation Summary Form

AO 97-OSS-03	Small Explorer Program and Missions of Opportunity

Principal Investigator Professor Robert P. Lin		
Department Space Sciences Laboratory		
Company/Institution University of California, Berkeley		
Street Address Centennial Drive at Grizzly Peak Boulevard		City/Town Berkeley
State California	Zip/Postal 94720-7450	Country USA
Telephone (510)642-1149	Fax (510)643-8302	E-Mail Address rlin@sunspot.ssl.berkeley.edu

Proposal Title
The High Energy Solar Spectroscopic Imager (HESSI)

Science Theme Supported (1 = primary; 2 = secondary)
- [ ] Structure and Evolution of the Universe
- [1] The Sun-Earth Connection
- [ ] Astronomical Search for Origins and Planetary Systems

Abstract (Limit 150 words)

HESSI will investigate the physics of particle acceleration and energy release in solar flares. Observations will be made of X-rays and gamma rays from 3 keV to 20 MeV with an unprecedented combination of high resolution imaging and spectroscopy. HESSI uses Fourier-transform imaging with 9 bi-grid modulation collimators and cooled germanium detectors mounted on a Sun-pointed spin-stabilized spacecraft in a low-altitude orbit with an inclination of 38°. It will provide the first imaging spectroscopy in hard X-rays with ~2 arcsecond angular resolution, time resolution to tens of ms, and ~1 keV energy resolution; the first gamma-ray line spectroscopy with ~2-5 keV energy resolution; and the first gamma-ray line and continuum imaging with ~36-arcsecond angular resolution. HESSI is planned for launch by July 2000, in time to detect the thousands of flares expected during the next solar maximum.

Small Explorer and Missions of Opportunity
Investigation Summary Form (Page 2)

Principal Investigator
Professor Robert P. Lin
Proposal Title
The High Energy Solar Spectroscopic Imager (HESSI)

Mission Mode (Check one)	Cost (FY97$)	
[X]Small Explorer	NASA Mission Cost	$66.7 million
[ ]Mission of Opportunity	Total Mission Cost	$72.2 million

Anticipated Launch Vehicle:
SELVS-II, Payload Envelope A

Co-Investigator(s) at Other Institutions		
Name	Institution	E-mail
Dr. Brian R. Dennis	NASA Goddard Space Flight Center	Brian.R.Dennis.1@gsfc.nasa.gov
Dr. Carol Jo Crannell	NASA Goddard Space Flight Center	Carol.J.Crannell.1@gsfc.nasa.gov
Dr. Gordon D. Holman	NASA Goddard Space Flight Center	Gordon.D.Holman.1@gsfc.nasa.gov
Dr. Reuven R. Ramaty	NASA Goddard Space Flight Center	Reuven.R.Ramaty.1@gsfc.nasa.gov
Dr. Tycho T. von Rosenvinge	NASA Goddard Space Flight Center	tycho@lheamail.gsfc.nasa.gov
Prof. Richard C. Canfield	Montana State University	canfield@isass6.solar.isas.ac.jp
Prof. A. Gordon Emslie	University of Alabama in Huntsville	emslieg@email.uah.edu
Dr. Hugh S. Hudson	Solar Physics Research Corporation	hhudson@solar.stanford.edu
Dr. Gordon J. Hurford	California Institute of Technology	gh@sundog.caltech.edu
Mr. Norman W. Madden	Lawrence Berkeley National Laboratory	
Prof. H. Frank van Beek	Delft University of Technology, The Netherlands	fvanbeek@worldaccess.nl
Co-Investigators not funded by NASA		
Prof. Arnold Benz	Institute of Astronomy ETHZ, Switzerland	abenz@solar.stanford.edu
Dr. Patricia L. Bornmann	National Oceanic and Atmospheric Administration	pbornmann@solar.stanford.edu
Prof. John C. Brown	University of Glasgow, Scotland, UK	john@astro.gla.ac.uk
Dr. Shinzo Enome	National Astronomical Observatory, Japan	enome@hotaka.mtk.nao.ac.jp
Dr. Takeo Kosugi	National Astronomical Observatory, Japan	kosugi@laputa.mtk.nao.ac.jp
Dr. Nicole Vilmer	Observatoire de Paris-Meudon, France	vilmer@obspm.fr
Dr. Alex Zehnder	Paul Scherrer Institut, Switzerland	Alex.Zehnder@psi.ch

Research Proposal to the
National Aeronautics and Space Administration

submitted by

The Regents of the University of California
Space Sciences Laboratory
c/o Sponsored Projects Office:
University of California, Berkeley
Attn: Joyce B. Freedman, Director
Sponsored Projects Office
336 Sproul Hall # 5940
Berkeley, CA 94720-5940
(510) 642-8110; fax (510) 642-8236
jbfreed@uclink2.berkeley.edu

UCBSSL 1925/97

Proposal in Response to AO 97-OSS-03:

THE HIGH ENERGY SOLAR SPECTROSCOPIC IMAGER (HESSI)

Principal Investigator

Prof. Robert P. Lin
University of California, Berkeley
Space Sciences Laboratory # 7450
Berkeley, CA 94720-7450
(510) 642-1149; fax (510) 643-8302
rlin@ssl.berkeley.edu

Co-Investigators at Other Institutions

See Investigation Summary Form

Period of Performance

October 1, 1997 - July 31, 2003

Proposed Costs (FY97$)

NASA Mission Cost: $66.7M
Total Mission Cost: $72.2M

June 15, 1997

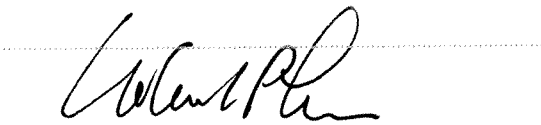

Robert P. Lin
Principal Investigator, and
Associate Director
Space Sciences Laboratory

Joyce B. Freedman
Director
Sponsored Projects Office

C. TABLE OF CONTENTS

List of Figures

Section D

List of Tables

D. SCIENCE

Summary. **The primary scientific objective of the High Energy Solar Spectroscopic Imager (HESSI) is to understand particle acceleration and explosive energy release in the magnetized plasmas at the Sun, processes which also occur at many other sites in the universe.** The Sun is the most powerful particle accelerator in the solar system, accelerating ions up to tens of GeV and electrons to hundreds of MeV. Solar flares release up to 10^{32}-10^{33} ergs in 10^{2}-10^{3} s. The accelerated 10-100 keV electrons (and possibly >~1 MeV/nucleon ions) appear to contain a significant fraction, perhaps the bulk, of this energy, indicating that the particle acceleration and energy release processes are intimately linked. How the Sun releases this energy, presumably stored in the magnetic fields of the corona, and how it rapidly accelerates electrons and ions with such high efficiency, and to such high energies, is presently unknown.

The hard X-ray/γ-ray continuum and γ-ray lines are the most direct signatures of energetic electrons and ions, respectively, at the Sun. **HESSI will provide the first hard X-ray imaging spectroscopy, the first high-resolution spectroscopy of solar γ-ray lines, the first imaging above 100 keV, and the first imaging of solar γ-ray lines.** HESSI combines an imaging system consisting of 9 rotating modulation collimators (RMCs), each with a high-spectral resolution germanium detector (GeD) covering energies from soft X-rays (3 keV) to high-energy γ-rays (20 MeV). HESSI's hard X-ray imaging spectroscopy provides spectral resolution of ~1 keV, spatial resolution down to ~2 arcsec, and temporal resolution as short as tens of milliseconds. **These parameters are, for the first time, commensurate with physically relevant scales for energy loss and transport of the >~10 keV electrons that are believed to contain much of the energy released in the flare.**

HESSI's γ-ray imaging spectroscopy will provide **the first imaging of energetic protons, heavy ions, relativistic electrons, neutrons, and positrons; the first information on the angular distribution of accelerated ions; and detailed information on elemental abundances for both the ambient plasma and the accelerated ions.**

With the fleet of spacecraft (SOHO, Wind, ACE, Ulysses, TRACE, GOES, Yohkoh, SAMPEX, CGRO, etc.)[1] that will already be in place, **a HESSI launch in mid-2000 would provide the crucial missing high energy measurements needed for comprehensive studies of the solar maximum.**

A two-year nominal mission (a third year is highly desirable) will provide **observations of tens of thousands of microflares, thousands of hard X-ray flares, and of order a hundred γ-ray line flares.** Rapid, direct access by the solar scientific community to the HESSI data and analysis software, together with **a U.S. Guest Investigator program funded from HESSI MO&DA funds, plus extensive foreign participation,** will ensure the maximum scientific return from this comprehensive data set.

HESSI will also obtain **hard X-ray imaging of the Crab Nebula with ~2 arcsec resolution,** and monitor a large fraction of the sky to provide, serendipitously, **high spectral resolution observations of transient hard X-ray and γ-ray sources,** including accreting black holes, cosmic γ-ray bursts, and terrestrial bursts from relativistic electron precipitation, aurora, and lightning.

HESSI's full-Sun field of view and storage of all information from every photon in a solid-state memory (sized to hold all the data from the largest flare) mean that flare data will rarely be lost and that mission operations can be automated. A 600-km altitude, 38° inclination circular orbit is baselined to allow uplink/downlink to a single ground station co-located with the Mission/Science Operations Center at the PI institution.

The extensive heritage from the UCB HIREGS and GSFC HEIDI balloon programs, and the UCB/GSFC FAST SMEX program, and recent NASA-funded technology development efforts, enable the HESSI instrument to be built with **no new development**. Spectrum Astro, our industry partner, will provide a simple, reliable, and inexpensive Sun-pointed spin-stabilized spacecraft based on subsystems already developed and flight-qualified from the Lunar Prospector, MSTI, MightySat, New Millenium, and FAST/-SMEX programs. Thus **HESSI is ready to be built within the SMEX cost and schedule constraints for launch in mid-2000.**

[1] See List of Acronyms in Appendix I-4.

The proposed mission concept has been endorsed by numerous advisory groups (e.g., NASA's Space Sciences Advisory Committee, and the National Academy of Science's Committees on Solar and Space Plasmas and on Solar Terrestrial Research), and was selected as a MIDEX alternate.

The HESSI team includes leading experts in solar high-energy spectroscopy and imaging, with decades of space hardware and data analysis experience. The team is committed to educational and public outreach, and has an outstanding record of involving young scientists/engineers, both graduate and undergraduate, as well as high school students and teachers.

D.1 Scientific Goals and Objectives

The processes of particle acceleration and impulsive energy release occur in active cosmic plasmas at diverse sites throughout the universe, ranging from planetary magnetospheres to active galactic nuclei. The understanding of these processes is a major goal of space physics and astrophysics, but we are just beginning to perceive the relevant basic physics. The Sun constitutes an unparalleled laboratory for investigating these processes. Its proximity allows measurements over the entire wavelength range to be made on physically relevant scales. At the same time, the system as a whole can be studied, and escaping energetic particles and plasma can be sampled directly. Further, the complexity of solar magnetic fields and the solar atmosphere leads to a broad range of acceleration phenomena, mirroring the rich diversity of processes occurring on cosmic scales.

Solar flares are the most explosive of these phenomena. **High-energy emissions are the most direct signature of the acceleration of electrons, protons and heavier ions in solar flares.** The hard X-ray and γ-ray continuum is produced as bremsstrahlung by energetic electrons. Nuclear collisions of energetic ions with the ambient solar atmosphere result in a complex spectrum of narrow and broad γ-ray lines that contain unique information on not only the accelerated ions but also the ambient solar atmosphere.

HESSI will have sensitivity and dynamic range sufficient to provide meaningful observations from microflares and the earliest emissions from a flare, to the peaks of the largest flares. The high spectral and spatial resolution of these observations will permit, for the first time, the deciphering of the rich information encoded in both the γ-ray lines and the highly structured photon continuum. These high-energy emissions are accompanied by longer wavelength emissions, and sometimes by escaping energetic particles. Their observation by the fleet of spacecraft that will already be in place, and by ground based instruments, will provide the crucial information on the context in which the high energy processes occur.

Particle Acceleration and Energy Release. Bursts of hard X-rays (>~20 keV) are the most common signature of the impulsive phase of a solar flare (Fig. D-1). These X-rays are bremsstrahlung, produced by accelerated electrons colliding with the ambient solar atmosphere. If these electrons are indeed nonthermal (i.e., electron energy $E_e >> kT$ of the ambient gas), then the energy lost by the electrons to bremsstrahlung in collisions with ambient ions is only a small fraction ($\sim 10^{-5}$) of their energy lost to Coulomb collisions with ambient thermal electrons. This inefficiency means that, for many flares, the energy in accelerated >20 keV electrons must be comparable to the total flare radiative and mechanical output (Lin and Hudson 1976). Thus the acceleration of electrons to tens of keV may be the most direct consequence of the basic flare-energy release process.

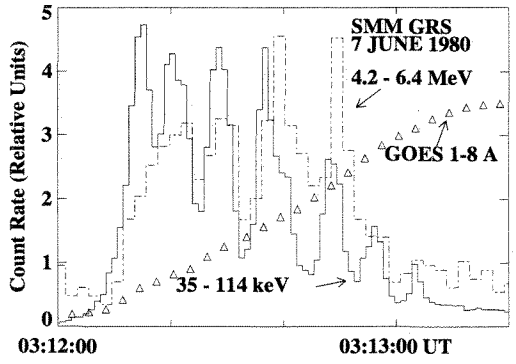

Figure D-1. Time profiles for a flare showing near-coincidence impulsive peaks in 35-114 keV hard X-rays (from energetic electrons) and 4.2-6.4 MeV γ-rays (from energetic ions).

It is, however, still possible that a fraction of the hard X-rays at tens of keV is quasi-thermal, i.e. produced by a Maxwellian population of electrons with $E_e \approx kT$ with $T >\sim 10^8$ K. Then the energy lost by one electron in an electron-electron Coulomb collision simply

increases the energy of the other. In that case, the principal losses are due to conduction and convection, which can be considerably less than the collisional losses in nonthermal models. **HESSI will determine the relative contribution of thermal and nonthermal emission to the hard X-ray spectrum.**

Hard (>20 keV) X-ray microflares, 10-100 times less intense than small flares, occur every ~5 minutes (Lin et al. 1984) near solar maximum, with the smaller ones occurring more frequently. Recently, high sensitivity measurements down to ~8 keV with the CGRO BATSE experiment show that solar impulsive bursts are observed >~3 times more often above 8 keV than above 25 keV (Lin 1997). Essentially every active region transient brightening in thermal soft X-rays (Shimizu, 1995) is accompanied by an impulsive, nonthermal >8 keV burst. This suggests that the flare process may be a fundamental way by which stored magnetic energy is transiently released in the Sun's corona (Parker 1988). If the nonthermal spectra extend down to ~5 keV, the average rate of energy deposition by microflare accelerated electrons, assuming nonthermal X-ray production, could be a significant fraction of that required to heat the active region corona. **HESSI's high sensitivity imaging spectroscopy extending down to ~3 keV will allow the systematic survey of the microflare non-thermal contribution to coronal heating.** At the same time these "simple" microflares may provide unique insights into the basic flare acceleration and energy release processes.

Non-Relativistic Electron Acceleration. During the flare impulsive phase, the Yohkoh Hard X-ray Telescope (HXT) often observes double footpoint structures (Fig. D-2), with the two footpoints brightening simultaneously to within a fraction of a second (Sakao et al. 1994). These coincide, spatially and temporally, with Hα and white-light brightenings.

For some flares occurring near the solar limb, HXT has detected a co-temporal, weaker, hard X-ray source in the corona (Masuda et al. 1994; Alexander and Metcalf, 1997) *above* the soft X-ray loop linking the hard X-ray footpoints (Fig. D-2). This source has been interpreted as evidence for energy release by magnetic reconnection in a region above the soft X-ray loop.

Very rapid transport of energy from the release site down to the footpoint interaction regions is required. This can only be achieved by fast electrons streaming down the loop and depositing their energy in lower coronal and chromospheric footpoints, implying that nonthermal, tens of keV electrons are interacting with a cool ($T<10^5$ K) environment. The resulting heating of the ambient gas leads to evaporation of chromospheric material and flare radiation in the visible, UV/EUV and soft X-rays. Hard X-ray studies of electron time-of-flight (Aschwanden et al. 1996a,b,c) further support this nonthermal thick target model, but it is unclear how the implied huge currents (up to 10^{36} electrons/s or 10^{17} amps) can conform to the global electrodynamic constraints of the flare environment (Miller et al. 1997). **HESSI's hard X-ray imaging, with much higher dynamic range and**

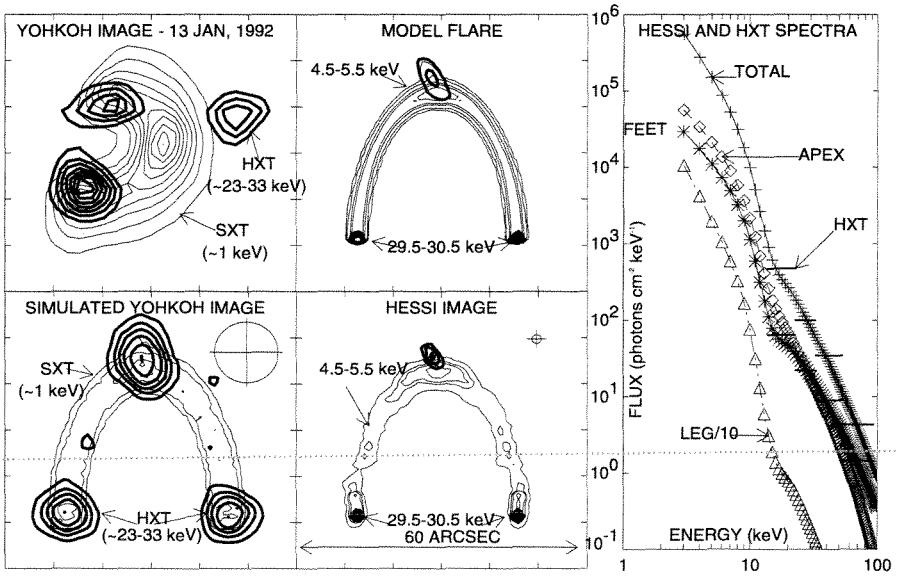

Figure D-2. *Top left*: The M1 limb flare seen with Yohkoh SXT and HXT. *Top center*: A model flare ten times more intense, expected to occur once a month on average at solar maximum. The thick and thin contours are for hard and soft X-rays, respectively. *Bottom*: Simulation results showing reconstructed images for Yohkoh (*left*) and HESSI (*center*), with point-spread function (50%) indicated. *Right:* Spectra at different locations with HESSI's spectral resolution and with the four HXT energy channels. Note that HESSI (but not HXT) has sufficient dynamic range capability (up to 100:1) to obtain spectra from the legs of the loop in the presence of the bright footpoints.

temporal and spectral resolution than Yohkoh HXT, is needed to study these coronal sources and electron streaming in detail.

Comparisons of microwave images with Yohkoh HXT images show a striking tendency for flares with three footpoints, i.e. in which two loops of different sizes appear to share a common footpoint (Nishio et al. 1997), suggesting loop-to-loop interactions. Typically the two loops have quite disparate sizes, with the longer loop (remote footpoint) initially visible only in hard X-rays. **HESSI's full-Sun observations, with high spatial and temporal resolution and wide dynamic range, are key to understanding the energy release in loop-loop interactions.**

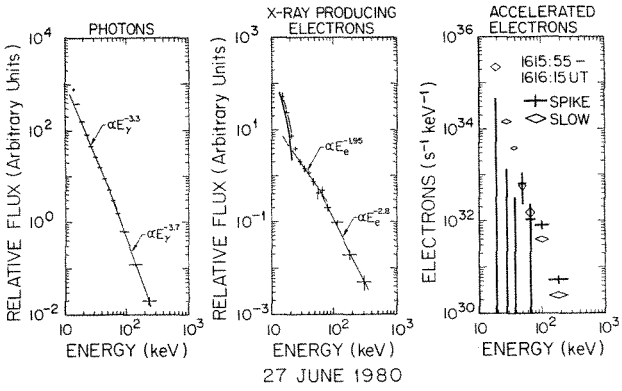

Figure D-3. High-resolution X-ray spectrum for 27 June 1980 flare (*left*) with the derived spectra of the X-ray producing electrons [N(E)] (*center*) and the accelerated electrons [F(E)] (*right*) (from Johns and Lin 1992).

As we show below, **high resolution X-ray imaging spectroscopy is the key to understanding the acceleration and energy release processes.** Precise measurements of the solar flare hard X-ray spectrum can be directly inverted to obtain the detailed spectrum of the parent X-ray-producing electrons at the Sun. The scintillation (NaI or CsI) detectors used for all previous spacecraft solar hard X-ray observations are inadequate for this task, but cooled GeDs with their near delta-function response for continuum measurements are ideal.

The first (and only) high-spectral resolution hard X-ray measurement, obtained with a balloon-borne GeD spectrometer on 1980 June 27 (Fig. D-3, left), immediately led to the discovery of a "superhot" ~3.5 x 10^7 K thermal source (Lin et al. 1981). It also showed that the nonthermal component does not fit a single power law or a single temperature thermal, but has a relatively sharp break at ~50 keV.

Johns and Lin (1992) showed that these data can be numerically inverted to determine N(E,t), the parent electron spectrum (Fig. D-3, center). N(E,t) is the result of modification of the ***accelerated*** electron spectrum F(E,t) by electron energy loss, propagation, and escape processes. Assuming that Coulomb collisions dominated these loss processes, Lin and Johns (1993) derived F(E,t) and found two separate components of accelerated electrons: an impulsive spike component with a spectrum peaked at ~50 keV, plus a slowly varying component with a power-law spectrum extending down to ~20 keV (Fig. D-3, right).

The peak in the spike electron spectrum suggests acceleration by a DC electric field, with the peak energy corresponding to the total potential drop in the field; such electron spectra are observed in the Earth's auroral zone. Comparison of the observed thermal "superhot" and nonthermal hard X-ray spectra with a model of heating and runaway electron acceleration in a DC electric field (Benka and Holman 1994) allowed determination of the electric-field strength, plasma density, and temperature in the flare.

HESSI will provide the crucial key for determining the particle acceleration process, namely the spectral, spatial, and temporal variation of the accelerated electrons, F(E,r,t). The 2-arcsec and tens-of-millisecond resolutions of HESSI are commensurate with the spatial and temporal scales for the accelerated electrons to lose their energy in the lower corona and upper chromosphere (ambient densities below ~10^{12} cm^{-3}). With HESSI's high energy resolution, the photon spectrum in each spatial and temporal element can be directly inverted to obtain N(E,**r**,t), the X-ray producing electron number density, as a function of energy (E), position (**r**), and time (t).

N(E,**r**,t), together with information on ambient density, magnetic field strength and topology, will allow the electron loss processes to be directly evaluated. This will decide whether the X-ray emission is thermal or nonthermal, since the energy loss characteristics of the emitting electrons are so different in the two cases. Then, via transport calculations (using a spatially dependent continuity equation including loss processes), the spatially and temporally resolved accelerated electron source distribution,

F(E,**r**,t), can be obtained. Once N(E,**r**,t) and F(E,**r**,t) are obtained, detailed quantitative models of the acceleration, energy release, and energy propagation processes can be constructed and tested. **This powerful technique is generally applicable to HESSI's hard x-ray continuum measurements.**

Non-imaging hard X-ray observations have already shown, via limb occultation, that the upper corona may be the source of hard X-ray emission of a different type (Hudson 1978), which may continue for tens of minutes (Cliver et al. 1986) and extend to altitudes of some 160,000 km (Kane et al. 1992). This emission could require as many as 10^{39} electrons above 5 keV with a total energy of 10^{31} ergs in a volume 10^{30} cm^3. **HESSI will provide N(E,r,t) for this source to decide whether it is related to the passage of shocks through the corona.**

Solar Energetic Particle (SEP) events observed in the interplanetary medium (IPM) are of two types, impulsive and gradual, so-called because of the temporal behavior of the associated flare soft X-ray burst (Lin 1987, 1994). **Impulsive SEP events** (~10^3/year at solar max) are rich in ~1-10^2 keV electrons and ^{3}He (Reames et al. 1985), with enhanced abundances of heavy ions (Fe, Mg, Si, S) and high ionization states (e.g. Fe^{+20}), suggesting high temperatures or stripping.

These events are generally associated with small flares, and solar type III radio bursts. The electrons escaping through the corona and IPM generate plasma waves, which, in turn, combine to produce the radio emission (see Lin 1990 for review). How the electron beam can propagate to >~1 AU without losing all its energy to the plasma waves is not known. Soft X-ray jets, recently discovered by Yohkoh (Shibata et al. 1992) turn out to be the dense channels in which some type III bursts propagate (Kundu et al. 1995). The spectra of the escaping type III electrons observed in the IPM are power-laws extending down to ~1 keV before a turnover, indicating a high coronal origin (Lin et al. 1996). **Comparisons of HESSI's determination of N(E,r,t) at the Sun down to a few keV with soft X-ray images and electron measurements in interplanetary space will help in understanding the electron acceleration, escape, and radiation processes, as well as the origin of the ^{3}He enhancements.**

Relativistic Electron Acceleration. Relativistic electrons have been detected in solar flares by observations of bremsstrahlung continuum emission extending up as high as several hundreds of MeV. At energies of a few hundred keV the spectrum often shows a flattening, indicating that a different mechanism may be accelerating the relativistic electrons. **HESSI will provide the first imaging in the energy range above 100 keV.**

Electrons of energies from a few hundred keV to several MeV also produce gyrosynchrotron radiation in the microwave and mm-wave region. Recently, impulsive spikes of mm-wave emission, implying relativistic electron acceleration, were detected by BIMA for even small flares (Kundu et al. 1990). Because the ratio of the magnetic field to the ambient density is much higher in the coronal part of loops than in the footpoints, the centroids of the microwave and soft γ-ray sources will likely be spatially distinct. **Comparison of N(E,r,t) obtained by HESSI with the spatial distribution, fluxes, and spectra of the microwaves and mm-waves, will provide information on the angular distribution of the electrons, on the magnetic field strength, and on the acceleration, trapping, and precipitation of the electrons.**

Ion Acceleration. Near the Sun, nuclear collisions of accelerated protons, α-particles, and heavier nuclei with the ambient solar atmosphere result in a rich spectrum (Fig. D-4 and Table D-1) of lines (Ramaty and Murphy 1987). γ-ray line emission has been observed from many solar flares, mostly by the Solar Maximum Mission (SMM) (Chupp 1990; Share and Murphy 1995). Energetic protons and α-particles colliding with carbon and heavier nuclei produce narrow de-excitation lines (widths of ~ few keV to ~100 keV), while energetic heavy nuclei colliding with ambient hydrogen and helium produce much broader lines (widths of a few hundreds keV to an MeV). Neutron capture on hydrogen and positron annihilation produce narrow lines (at 2.223 MeV and 0.511 MeV, respectively) which are delayed. **HESSI will probe ion acceleration with the first high-resolution spectroscopy of solar flare γ-ray lines and the first imaging of solar flare γ-rays.** HESSI's GeDs can spectrally resolve all the expected lines except the 2.223-MeV line (see foldout Fig. D11-J at end of section); none of these lines have been resolved by the solar γ-ray detectors to date.

Table D-1. HESSI response for γ-ray lines from a large flare (4 June 1991), and 3σ sensitivities (4th column).

Line Energy (MeV)	Excited Nucleus	Width (keV)	3σ Line Fluence (ph/cm²)	Large Flare			
				Line Fluence (ph/cm²)	HESSI Line Counts	HESSI Continuum Counts*	Number of σ
Prompt lines							
0.339	^{59}Ni	4	1.6	9.2	1512	37475	7.7
0.429†	^{7}Li	5	2.4	9.5	838	15839	6.5
0.478†	^{7}Be	10	3.5	9.5	854	25342	5.3
0.452†	^{7}Li-^{7}Be	30	2.3	19.0	3195	89004	10.5
0.847	^{56}Fe	5	1.4	17.3	1074	4471	14.4
0.932	^{55}Fe	5	1.2	2.5	274	3193	4.7
1.369	^{24}Mg	16	1.7	25.5	1567	6995	16.9
1.634	^{20}Ne	20	1.6	75.3	4297	6863	40.7
1.778	^{28}Si	20	1.9	30.4	1446	5245	17.7
2.618	^{20}Ne	60	3.5	11.4	445	4187	6.5
4.439	^{12}C	145	6.9	73.3	1294	5383	15.8
6.129	^{16}O	145	11.4	57.6	549	2716	9.6
Delayed lines							
0.511	e^+/e^-	5	2.4	196.9	21060	15432	110.2
2.223	^{2}H	2.5‡	0.6	298.7	13345	346	114.1

* For most lines, about 90% flare continuum and 10% instrumental background for this bright flare.
† The narrow lines are for a downward beam or a fan beam; the single broad line at ~0.45 MeV is for an isotropic distribution.
‡ This line has an intrinsic width of ~0.1 keV, so we used the instrument FWHM resolution (2.5 keV).

HESSI will provide the first determination of line shapes, which are direct probes of the angular distribution of the interacting accelerated ions. The derived angular distributions will discriminate between various transport and acceleration mechanisms. For example, ions which suffer strong pitch-angle scattering into loss cones due to plasma turbulence in the coronal part of the loops will mostly interact while going downward and produce different line shapes than ions which interact while mirroring near the loop footpoints.

The shape of the 0.511 MeV positron annihilation line gives information about the ambient medium since the positrons slow down before annihilating. **HESSI's energy resolution at 0.511 MeV is sufficiently good to measure temperatures down to 10^4 K,** and it can easily distinguish among annihilation sites located below the transition region, in the corona, or in the hot (~10^7 K) flare plasma. The bulk of the annihilations would occur in the corona if the magnetic field traps the positrons there. Measurements of a positronium continuum below 0.511 MeV (from 3-photon decay), which is prominent only if the density of the ambient medium is less than ~10^{15} cm^{-3} (Crannell et al. 1976), will show whether energetic ions have penetrated to regions of high density (Hua et al. 1989).

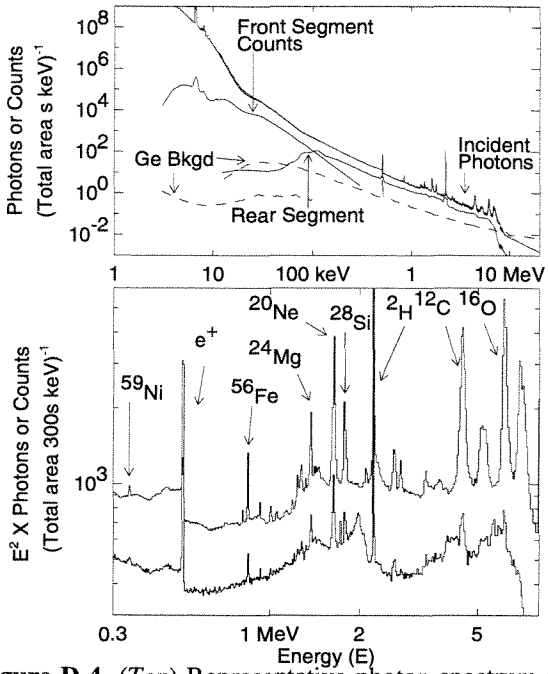

Figure D-4. (*Top*) Representative photon spectrum for a large X-class flare (such as 4 June 1991) over the HESSI energy range. Also shown are the corresponding count-rate spectrum (lower curve) and expected background. (*Bottom*) Expanded γ-ray line region (× E^2). The line response above 4 MeV is much weaker because the photopeak efficiency drops. The broad feature at 1.9 MeV is Compton backscatter of 2.2 MeV.

HESSI has a unique capability to image in narrow γ-ray lines, where line counts dominate over the background (Table D-1). Thus, both the 2.223 MeV neutron capture and 0.511 MeV positron annihilation lines can be imaged. Although γ-ray lines have never been directly imaged, the 2.223 MeV line was once detected in a behind-the-limb flare (Vestrand & Forrest 1993). This line is formed when thermalized neutrons are captured by ambient protons in the photosphere, at a much greater depth than that at which nuclear reactions take place. Because of the very strong expected attenuation, the neutrons must have been produced by charged particles interacting on the visible hemisphere of the Sun. Thus, either the acceleration site was far removed from the optical flare site, or the charged particles were transported over large distances.

The continuum above 1 MeV (especially 4-7 MeV) is often dominated by the broad lines from accelerated heavy (Z>2) ions, and can be mapped to localize them. In a large γ-

ray line flare with good statistics, the >3 MeV protons can be located by imaging the ^{20}Ne de-excitation line. Locations and source sizes will be determined in large flares to ~35 arcsec, allowing footpoints to be identified. **HESSI's γ-ray images will provide crucial information on acceleration and transport of energetic heavy ions and protons.**

HESSI's high energy resolution allows it to separate closely spaced lines (e.g. 1.634 and 1.778 MeV), but more importantly it dramatically increases the sensitivity for detecting very narrow lines (e.g., the 2.223 MeV line). By observing the ratio between the 2.223 MeV line and the bremsstrahlung continuum in many flares, **HESSI will test whether ions are accelerated in all flares, down to much lower flux thresholds** than with SMM.

The bulk of the γ-ray line emission is produced by ions with energies of 10-100 MeV/nucleon that contain only a small fraction of the energy in the ~>20 keV electrons. However, systematic study of SMM γ-ray line flares (Share and Murphy 1995) shows that the 1.634 MeV ^{20}Ne line is unexpectedly enhanced. Because the cross section for ^{20}Ne has an unusually low energy threshold (~2.5 MeV), this effect may be due to large fluxes of low-energy ions with a total energy content perhaps comparable to that in accelerated electrons, rather than to an overabundance of neon (Ramaty et al. 1995; Emslie et al. 1997). **HESSI will provide the first high-resolution spectroscopy and imaging of the ^{20}Ne line.** The ratio of the flux in this line to other lines will probe the ion energy spectrum (and total ion energy content) down to ~1 MeV.

If DC electric fields accelerate the hard-X-ray-producing electrons, then they may also accelerate many 100-keV protons (Holman 1995). Optical Hα polarization is highly sensitive to low-energy (100 keV) protons. Positive detections of Hα polarization in a few flares have been made (Henoux et al. 1990), but their interpretation is uncertain. With simultaneous HESSI ion and electron images and Hα polarization maps, **the partition of energy between accelerated electrons (derived from hard X-ray measurements) and ions may be measured for the first time.**

A very important discovery during Cycle 22 was that of long-duration γ-ray emission. GeV γ-rays from pion decay were observed with EGRET on CGRO for up to 8 hours after the impulsive phase of the 11 June 1991 flare (Kanbach et al. 1993). Nuclear line emission at 2.223 MeV was also observed with essentially the same time profile (Rank 1996). This strongly suggests that acceleration to GeV energies was ongoing for a very long time. With its sensitivity, **HESSI will observe the 2.223-MeV line for several hours after a flare similar to the 11 June flare.** These observations will address the issue of particle trapping vs. continuous acceleration in flares.

Time variation of the 2.223-MeV line can also be used to determine the unknown ^{3}He abundance in the photosphere. ^{3}He has a very high cross section for neutron capture and removes neutrons from the population which produces the 2.223 MeV line. Not only is the line flux reduced, but its time profile is changed in a way that can be compared to models (Hua & Lingenfelter 1987). The solar ^{3}He abundance is essential for studies of galactic abundance evolution and may have cosmological implications. Even though the coronal ^{3}He/^{4}He ratio is measured in the solar wind, the γ-ray observations provide a direct measure of the photospheric abundance.

Alpha particle interactions with ambient He produce ^{7}Be and ^{7}Li in excited states leading to line emission at 0.429 and 0.478 MeV. SMM detected larger-than-expected fluences of these lines (Share & Murphy 1997; Mandzhavidze et al. 1997). Either the abundance of accelerated α-particles is higher than expected from SEP observations (Reames 1994), or the abundance of ambient helium is much higher than the photospheric values obtained from both helioseismology (Hernandez & Christensen-Dalsgaard 1994) and the standard solar model (Bahcall & Pinsonneault 1995). **HESSI can detect a narrow line at 339 keV due to the bombardment of ^{56}Fe by energetic α-particles leading to ^{59}Ni in an excited state (Fig. D-4). This will distinguish between enhanced α-abundance in accelerated particles or in the ambient medium.**

Acceleration due to gyroresonant interactions with plasma turbulence in impulsive flares is hypothesized to be responsible for the large e/p ratios and ^{3}He enrichments (Temerin and Roth 1991). The enrichment of heavy-element (in particular Fe) abundances in SEPs is another signature of impulsive flares (Reames et al. 1994). Also, SMM observations (Share & Murphy 1995) have shown that the abundance ratio of low FIP (Mg, Si, Fe) to high FIP (e.g., Ne) elements is en-

hanced in the de-excitation region relative to the photosphere (Ramaty et al. 1995), as is already is known for the corona from SEP measurements. **Comparing HESSI's γ-ray determination of e/p and elemental abundances (both in accelerated particles and in the ambient medium) at the Sun, with IPM measurements of the composition of SEPs will test the hypothesis that γ-ray flares and impulsive SEP events have a common origin** (Ramaty et al. 1993).

Large SEP Events. Gradual SEP events (tens per year at solar max) are generally large (hence also called LSEP) events dominated by protons, with "normal" solar abundance and ionization states typical of quiet 1-2 × 10^6 K corona, (e.g. Fe^{+13}). These are associated with large flares and fast Coronal Mass Ejections (CME's) driving shock waves in the IPM.

In the most intense LSEP events, the fluence of protons sufficiently energetic (>~50 MeV) to penetrate the walls of manned spacecraft is high enough to result in a harmful or even fatal radiation dose to astronauts. Such intense events also degrade electronic components on unmanned spacecraft. SEPs can also penetrate deep into the atmosphere over the Earth's magnetic polar regions and produce increased ionization, lowering the ionosphere and disrupting radio communications.

The >~50 MeV proton flux in classic LSEP events generally shows a rapid onset within about the particle travel time after a large flare, indicating that the acceleration occurred close to the Sun at about the time of the flare. LSEPs are thought to be accelerated by CME shocks close to the Sun (Reames 1996). In the IPM, however, CME shocks appear to accelerate particles only up to ~10 MeV, but not to >~50 MeV, unless an energetic seed population is already present.

Studies by the NOAA Space Environment Center (SEC) show that the best current predictor of LSEPs is the systematic spectral hardening with time of the flare hard X-ray burst (Kiplinger 1995). The soft X-ray long-duration events (LDE) associated with LSEP events appear to have hard X-ray emission in about the same proportion as in impulsive events (Dennis and Zarro 1993; Hudson et al. 1994). It is not clear how this LDE hard emission relates to the impulsive flare burst.

Recently, the SOHO EIT has observed the "Moreton wave" phenomenon of blast waves radiating directly from a flare site (Thompson et al. 1997). Shocks in the corona within about 3 solar radii produce metric type II solar radio bursts. These are flare-related and evidently not related to fast CMEs (Wagner and McQueen, 1983; Gopalswamy and Kundu, 1995; Gopalswamy et al. 1997). **HESSI hard X-ray and γ-ray spectroscopy and imaging, together with observations of coronal shocks, SEPs, and CMEs, are needed to understand the various ion acceleration processes at the Sun and their relationship to flare electron acceleration, and for more accurate prediction of LSEP events.**

Context Observations. For interpreting HESSI's observations, knowledge of the physical parameters in the regions of interest is essential. Imaging spectroscopy (down to 3 keV) by HESSI itself will reveal the temperature, density, location, and temporal evolution of flare thermal plasmas, as well as the characteristics of the low energy (<20 keV) accelerated electrons that may contain the bulk of the energy released.

The Soft X-ray Imager (SXI), to be launched in early 2000 on a GOES spacecraft (and SXT on Yohkoh if still operational), will provide broad-band (6-60 Å) images to determine the global and local morphology of coronal features.

SOHO's EIT and CDS will provide EUV images and spectra that give the temperature, emission measure, density, and velocity of plasma in the chromosphere, transition region, and corona at temperatures ranging from ~2 × 10^4 K to ~2 × 10^7 K. SOHO/LASCO will provide evolution, mass, momentum, and energy transport information on any coronal activity, particularly CMEs, that may result in particle acceleration. SOHO/MDI and ground-based instruments will provide measurements of magnetic field strengths in the photosphere.

SEP and solar wind composition measurements will be provided by Wind, ACE, SOHO, SAMPEX, and Ulysses. Wind and Ulysses also provide IP radio measurements. **For a HESSI launch in mid-2000 the required space context observations will be available from the spacecraft that will already be in place.**

Microwave and mm-wave imaging/ spectroscopy will provide direct measurements of preflare coronal magnetic fields plus thermal and nonthermal electron parameters. Vector magnetograms will show the role of evolving magnetic fields (e.g., emerging magnetic flux) and provide maps of electric

currents to define their relationship to sites of possible DC electric field acceleration (Canfield et al. 1993). Optical imaging spectra provide velocities in the lower atmosphere, a straightforward measure of the energy that goes into chromospheric evaporation. Multiband optical imaging will provide information on energy release, since the optical continuum emission is thought to be the largest component of the radiative energy budget of flares. Imaging Hα polarization measurements may provide a way to detect ~100 keV accelerated protons. **HESSI will provide support to ensure that key ground context observations of the needed quality are available**.

Non-Solar Science. Although designed as a solar instrument, HESSI provides a combination of ~keV resolution, ~150 cm^2 collecting area, and wide field of view (at 60°-120° to the solar direction) that makes it complementary to the ESA INTEGRAL mission, which will have a narrow field of view.

HESSI will be an effective high spectral resolution **hard X-ray/γ-ray all-sky monitor**, allowing identification of transients (black-hole X-ray novae, Be/neutron star binary outbursts, etc.) within days using occultation. It benefits from the spacecraft's rotation, which will produce many detector/detector occultations per minute, as well as from two brief Earth occultation periods per orbit (Harmon et al. 1992; Zhang et al. 1993). **HESSI will be able to resolve cyclotron absorption features from bright transients** such as A0535+26, and the line shapes will test models of the neutron star polar region. HESSI can also search for the line features between 10 and 100 keV reported by Ginga in **γ-ray bursts** but not confirmed by BATSE (Band et al. 1994), and study the Galactic positron annihilation and ^{26}Al decay lines on angular scales larger than the INTEGRAL field of view.

Once a year a small offset pointing of HESSI (<1°) would result in **imaging of the Crab Nebula** with unprecedented spatial (2 arcsec) and energy (~1 keV) resolution. Although the nebula shows intricate structure from radio through UV, with a tendency toward smaller sizes at higher energies, it has been imaged in hard X-rays only once (Pelling et al. 1987), with only 15 arcsec resolution and two energy bands. One day of HESSI observation would give ~2×10^5 source counts from 25-35 keV, for ~300 σ of total flux in the map. Maps could be made up to ~200 keV. Yearly maps can show changes; significant changes in structure have been seen in the radio and optical bands (Bietenholz & Kronberg 1992).

HESSI will also provide high spectral and temporal resolution measurements of terrestrial X-ray/γ-ray emissions from relativistic electron precipitation (Smith et al. 1995), auroral precipitation, and bursts associated with lightning (Fishman et al. 1994).

Expected Results. The total HESSI effective photopeak area (foldout Fig. D-11G) and response to a large flare (Fig. D-4 and Table D-1) were obtained with detailed Monte Carlo calculations, using the GEANT code and taking into account the grids and all known materials in the cryostat and detector modules. The orbit-average background (Fig. D-4) was similarly computed and is consistent with scaling from balloon-borne GeD measurements.

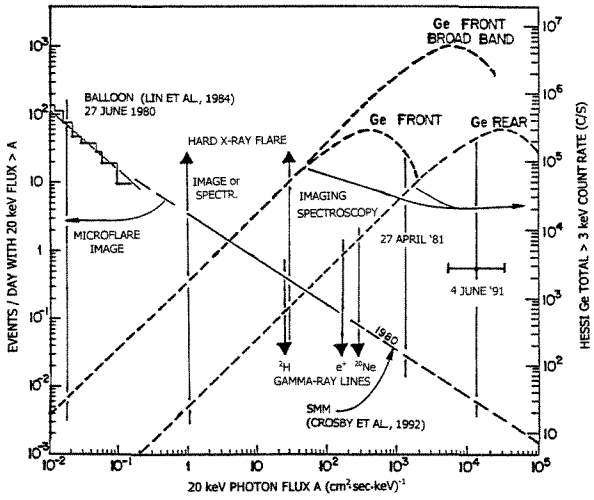

Figure D-5. Integral flare size distribution with 20 keV X-ray flux, for the flares and microflares observed in 1980; and corresponding HESSI total (9 GeDs) counting rates for front and rear segments.

The total count rates are shown in Fig. D-5 for the front and rear GeD segments. The turnover in the count rates at high photon fluxes are due to dead-time from the pulse pile-up rejection used to eliminate resolution degradation. Broadband imaging with ~10 keV resolution for the GeD front segment extends the dynamic range to a 20 keV X-ray flux of ~3×10^4 cm^{-2} s^{-1} keV^{-1}, while the GeD rear segment can handle flares with three times higher flux, or up to ~30 to ~100 times larger than the 27 April 1981 γ-ray line flare.

Thus, **HESSI is the first solar high energy instrument to have the dynamic range to both detect microflares and make quantitative spectral measurements of the largest flares.**

Assuming HESSI observes the Sun 60% of the time, and with the predicted HESSI background, ~10^2 microflares per day will be detectable above a 20-keV photon flux of ~5×10^{-3} photons cm^{-2} s^{-1} keV^{-1}. Since a minimum of about a hundred source counts is needed to form a simple image, the location and size of microflares could be determined for ~40 events/day, with fluxes about three times larger than threshold.

For ~2 events / day with >~10^3 counts s^{-1} above 15 keV, rapid spatial changes of the hard X-ray sources could be followed with simple images on time scales of 0.1 s, or full-Sun spectroscopic studies with no imaging (e.g., Lin and Johns 1993) could be carried out to obtain N(E,t). Detailed imaging spectroscopy providing N(E,**r**,t) could be done with images in each of ten energy intervals with ~2-s time resolution for one event every ~5 days with >~10^4 counts s^{-1} above 15 keV; crude imaging information could be obtained in tens of milliseconds.

Assuming that every flare accelerates ions with fluxes proportional to the hard X-ray flux, the calculated 3σ sensitivities (Table D-1) imply that the 2.223-MeV line should be detected, on average, once every ~4 days, the 0.511-MeV line every ~14 days, and prompt de-excitation lines every ~21 days.

The source location and size could be obtained every ~13 days for the 2.223-MeV line, and once every ~60 days for the 0.511-MeV line and the nuclear continuum from energetic heavy ions. Detailed spectroscopy revealing many γ-ray lines will be possible for these flares, allowing the abundances of many elements to be determined.

Every six months, a flare can be expected that is sufficiently large to locate the source of emission of narrow prompt de-excitation lines from energetic protons. Thus, **tens of thousands of microflares, thousands of hard X-ray flares, and of order a hundred γ-ray line flares will be detected in the HESSI 2-year operating lifetime.**

D.2. Science Implementation

D.2.a Instrumentation

The HESSI scientific objectives will be achieved with high resolution imaging spectroscopy observations from soft X-rays to γ-rays, utilizing a single instrument consisting of an Imaging System, a Spectrometer, and the Instrument Electronics. The Imaging System is made up of nine Rotating Modulation Collimators (RMCs), each consisting of a pair of widely separated grids mounted on a rotating spacecraft (Fig. D-11K). Pointing information is provided by the Solar Aspect System (SAS) and Roll Angle System (RAS) (Fig. D-11K,M).

The Spectrometer (Fig. D-11N) has nine segmented GeDs, one behind each RMC, to detect photons from 3 keV to 20 MeV. The GeDs are cooled to <~75 K by a space-qualified long-life mechanical cryocooler (Fig. D-11Q) to achieve the highest spectral resolution (Fig. D-11J) of any presently available γ-ray detector. As the spacecraft rotates, the RMCs convert the spatial information from the source into temporal modulation of the photon counting rates of the GeDs. The Instrument Electronics amplify, shape, and digitize the GeD signals, provide low-voltage power and GeD high voltage, format the data, and interface to the spacecraft electronics. Essentially all of the HESSI instrument components have extensive flight or life-cycle heritage (Table D-2).

Table D-2. HESSI Instrument Heritage

Spectrometer	
Germanium Detectors	HIREGS, HEXAGONE
Instrument Electronics	HIREX, HIREGS, FAST
Cryostat	HIREGS, HEXAGONE
Mechanical Cooler	GSFC life tests
Imaging System	
Grids	HEIDI, Test Grids
Metering Structure	GSFC Test Demo Unit, HEIDI
Solar Aspect System	HEIDI
Roll Angle System	Breadboard test
Spacecraft Interface	FAST
Flight Software	FAST, HIREGS

The energy and arrival time of every photon, together with SAS and RAS data, are recorded in the spacecraft's on-board 2-Gbyte solid-state memory (sized to hold all the data from the largest flare) and automatically telemetered within 48 hours. With these data, the X-ray/γ-ray images can be reconstructed on the ground (see example, Fig. D-11B,O,P). The instrument's ~1° field of view is much wider than the ~0.5° solar diameter, so all flares are detected, and pointing can be automated.

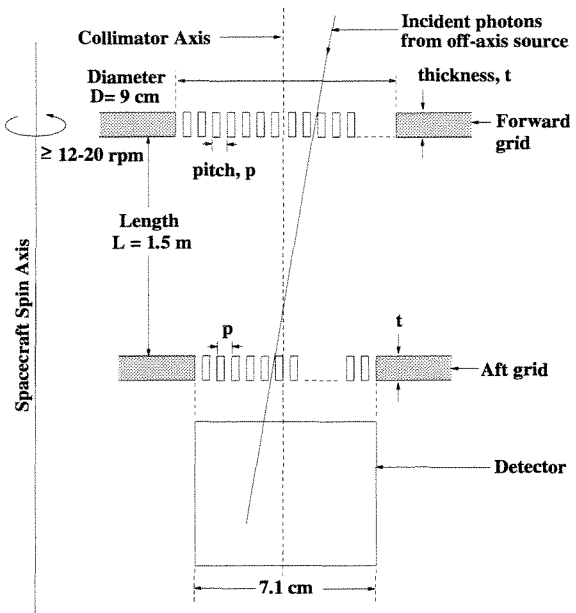

Figure D-6. Schematic showing the instrument parameters that define the imaging capability.

D.2.a.1. Imaging System

The only viable method of obtaining arcsecond-class images in hard X-rays and γ-rays within the SMEX constraints is to use Fourier-transform imaging. We use bigrid collimators consisting of a pair of widely separated grids in front of an X-ray/γ-ray detector (Fig. D-6). Each grid consists of a planar array of equally-spaced, X-ray-opaque slats separated by transparent slits. If the slits of each pair of grids are parallel to each other and if their pitches (p) are identical, then the transmission through the grid pair depends on the direction of the incident X-rays. For slits and slats of equal width, the transmission is modulated from zero to 50% and back to zero for a change in source angle to collimator axis (orthogonal to the slits) of p/L where L is the separation between grids (see Fig. D-6). The angular resolution is then defined as $p/(2L)$. For HESSI, the transmission of the source photons through the grids is modulated by mounting the instrument on a rotating spacecraft. The detector records the arrival time and energy of individual photons, allowing the modulated counting rate to be determined as a function of rotation angle. Note that **the detector does not need to have any spatial resolution and hence can be optimized for high sensitivity and energy resolution.**

For a parallel incident beam, the modulated waveform generated by a smoothly rotating spacecraft has a distinctive quasi-triangular shape (Fig. D-11O) whose amplitude is proportional to the intensity of the beam and whose phase and frequency depend on the direction of incidence. For complex sources, and over small rotation angles, the amplitude and phase of the waveform provide a direct measurement of a single Fourier component of the angular distribution of the source (e.g., Prince et al. 1988). Different Fourier components are measured at different rotation angles and with grids of different pitches.

For HESSI, the separation between grids in each RMC is L = 1.5 m and the grid pitches range from 34 μm to 2.75 mm in steps of $\sqrt{3}$ (see table of grid parameters – Fig. D-11F). This gives angular resolutions that are spaced logarithmically from 2.3 arcsec to >~3 arcmin, allowing sources to be imaged over a wide range of angular scales (Fig. D-11H). Diffuse sources larger than 3 arcmin are not imaged but full spectroscopic information is still obtained. Multiple smaller sources are imaged regardless of their separation.

In a half rotation (2 s) the 9 RMCs **measure amplitudes and phases of ~1100 Fourier components for a typical source location, compared to 32 Fourier components for the Yohkoh HXT, so far more complex flare images can be resolved.** Detailed simulations have been made of HESSI's response using image reconstruction techniques that have decades of heritage from the mathematically equivalent problem in radio interferometry. These show that **HESSI can obtain accurate images with a dynamic range (defined as the ratio of the brightest to the dimmest feature reliably seen in an image) of up to 100:1.** Fig. D-2 shows a simulation of an X1 flare similar in structure to that detected by Yohkoh, illustrating that **detailed high-resolution X-ray spectra can be obtained for each location in the image, thus providing true high-resolution imaging spectroscopy for the first time.**

Although one half rotation is required to measure a full set of Fourier components, the measurement of each component takes only a single modulation cycle, which is as short as 1.3 ms for the finest grids. Thus, when count rates are sufficiently high (>1000 c/s per detector), **crude images (from about ten Fourier components) can be obtained on timescales of tens of milliseconds.** The grids are oriented at large angles to each other to

optimize these fast images. If the source changes on these rapid timescales, space-time confusion can be avoided by using normalization techniques which exploit the fact that the modulation for each RMC occurs at a different rate.

The grid material and thicknesses can be chosen to provide modulation to energies as high as possible consistent with maintaining a ~1° FOV. We have chosen to have only two such maximum thickness grids, to provide γ-ray imaging while minimizing the loss in sensitivity for γ-ray line spectroscopy. Thus, with the grid parameters listed in Fig. D-11F, imaging is possible with 2.3 arcsec resolution to ~40 keV, 7 arcsec to ~400 keV and 36 arcsec to >10 MeV (Fig. D-11H). Even allowing for the grid absorption, the effective photopeak area for high resolution γ-ray spectroscopy is still ~80 cm^2 at 1 MeV (Fig. D-11G).

A detailed error analysis of the imaging performance has been carried out and the critical engineering requirements shown in Table D-3 were determined from a preliminary error budget. Changing the separation (L) between grids or displacing the grids parallel to the slits has little effect on imaging performance. A relative displacement perpendicular to the slits affects the phase but not the amplitude of modulation. Any such displacement will be accurately monitored by the SAS, and can be fully compensated for in the image reconstruction process.

The critical alignment requirement is associated with the rotation or *twist* of one grid with respect to the other about the line of sight to the source. A relative twist of p/D (D = diameter of grid) reduces the modulated amplitude almost to zero. Thus, the grid pairs must be well aligned in twist throughout the mission. For the finest grids (2 arcsec resolution) a 1-arcmin alignment is needed. Thus, **HESSI can achieve arcsec-quality images with an instrument having only arcmin alignment requirements**.

It should be noted that Fourier-transform imaging is a relatively "forgiving" process in that moderate alignment errors, even larger than the 3σ numbers in the error budget (Table D-3), generally only reduce the sensitivity of specific subcollimators and do not reduce the angular resolution. In-flight knowledge of these errors can be derived from the internal redundancy of the X-ray and SAS data, and applied to the collimator amplitudes and phases to recover most of the nominal telescope performance.

Table D-3. Critical Engineering Requirements

Factor	3σ Requirement	Blurring (arcsec) (FWHM)
Spacecraft Pointing [1]	<0.2°from Sun center	0
Aspect Error		
In rotating frame	1.5 arcseconds	1.2
In inertial frame	3 arcminute in roll	0.4
Absolute Solar Aspect[2]	1 arcsecond	0
Grid Imperfections[3]	4.5 microns	0.8
Grid Matching[4,5]	1 part in 3 x 10^4	0.5
Relative Twist[4]	1 arcminute	0.5

[1]Image quality is independent of spacecraft pointing provided that Sun center is kept within the 0.2° SAS field of view.
[2]Absolute solar aspect only affects image placement.
[3]Deviation of slit positions from their nominal location within a grid.
[4]Requirement scales linearly with grid pitch; the value given is for the finest grids.
[5]Matching of average pitch of the front and rear grid.

In practical terms, both Yohkoh HXT and SMM HXIS were coaligned to arcsecond precision using similar technology (Wülser et al. 1995; van Beek et al. 1980). Recent experience with HXT data analysis has shown how significant improvements in image quality can be achieved using the self calibration possible with in flight data. HESSI has the advantage that each RMC measures many Fourier components so that more extensive self-calibration will be possible, resulting in very high quality images.

Grids. Two different techniques will be used to fabricate the 9-cm diameter grids. For the finest two grid pairs, we will use photoetching. Three full-size, 25-μm thick, gold grids with the finest, 34-μm, pitch have been made at JPL (Fig. D-11D). The gold grids are supported on a 200-μm thick silicon substrate with a pattern of holes in it to allow X-rays down to ~3 keV through. These grids meet all our dimensional requirements for the two finest grid pairs.

For the coarser seven grid pairs, we will use stacking of tungsten blades with stainless-steel spacers in precisely machined Invar reference frames. This technique was developed and patented by Co-I van Beek. He has produced several test grids, including the over-sized 100-μm pitch grid (Fig. D-11E) that meets all requirements for Grid #3.

We have characterized both the JPL and the van Beek test grids using the GSFC Optical Grid Characterization Facility (OGCF), and subjected some of them to thermal cycling and launch-level vibration loads. As a result of these tests, we have established that **JPL and van Beek can make the grids we need to meet all of our science objectives.** Furthermore, **both JPL and van Beek have committed to meeting our schedule requirements.**

Metering Structure and Grid Trays. The critical alignment requirement for the metering structure is to maintain the relative twist of the finest grid pair to within one arcminute (Table D-3). **The proposed metering structure is based on the Telescope Demonstration Unit (TDU) built and tested at GSFC** (Fig. D-11C). The TDU's on-orbit alignment performance was simulated using SINDA thermal models and NASTRAN structural models. **The results of this analysis and the TDU thermal and vibration tests demonstrate that the proposed design satisfies all the mission requirements.**

To maintain alignment following thermal and vibrational stresses, flexural elements are used to mount the grids to the grid trays and the telescope tube to the spacecraft. This approach was demonstrated with the TDU and used successfully by Co-I van Beek in the Hard X-ray Imaging Spectrometer (HXIS) on SMM, where the alignment requirements were significantly more stringent. The fine grids will be precision aligned in twist by elastic deflection of these flexure elements.

Twist Monitoring System (TMS). Critical twist alignment will be monitored from initial assembly up to launch by the non-intrusive technique illustrated in Fig. D-11L. This was used successfully by Co-I van Beek to monitor the alignment of the X-ray collimators on the HXIS. The basic technique has been demonstrated at GSFC for digital readout by using a lensless CCD camera to determine the relative location of diffraction rings from the two alternately illuminated pin-hole sources. An easily measurable 1-μm change in the relative position of the diffraction patterns from the two pinhole/annulus combinations is produced by a 6-arcsec change in twist of one grid with respect to the other.

Solar Aspect System (SAS). The SAS provides (1) high-resolution, high-bandwidth aspect information for image reconstruction, (2) real-time aspect error signals for spacecraft pointing, (3) monitoring of the relative twist of the two grid trays, and (4) full-Sun white-light images for coalignment with ground-based images. The SAS is similar to the aspect system on HEIDI that demonstrated 0.5-arcsec performance at balloon altitudes. It consists of three identical lens-filter assemblies mounted on the forward grid tray to form full-Sun images on three 2048 x 13-μm linear diode arrays mounted on the rear grid tray (see Fig. D-11K and Fig. D-7). Simultaneous exposures of three chords of the focused solar images are made every 10 ms by each of the arrays. A digital threshold algorithm is used to select four pixels that span each solar limb for inclusion in the telemetry. These digitized pixel outputs allow six precise locations of the solar limb to be obtained on the ground by interpolation, thus providing knowledge of Sun center in pitch and yaw to 1.5 arcsec (3σ).

When the SAS is pointing to within ~0.2° of Sun center, simple algorithms using the limb pixel numbers also provide real-time error signals with ~<10 arcsec precision to the spacecraft Attitude Control System (ACS). Use of the SAS in this way for both imaging and pointing avoids problems of coalignment. The SAS is also used as a solar acquisition sensor with an effective radial field of view of 46 arcmin by the detection of a single limb in any one of the three diode arrays.

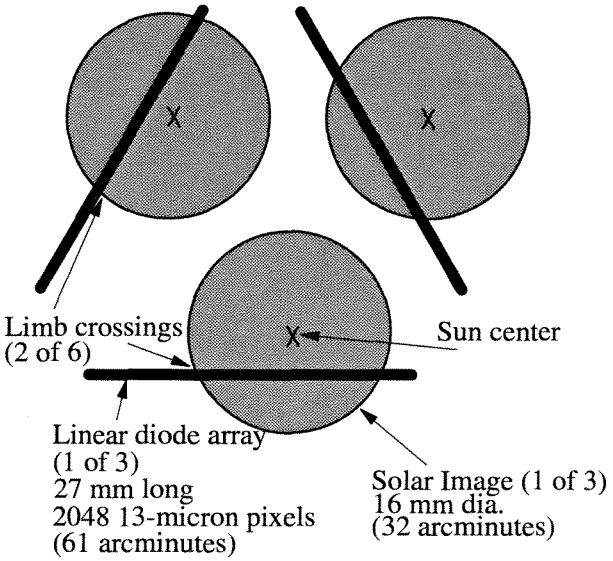

Figure D-7. Schematic illustrating the SAS principle of operation. The three linear diode arrays on the rear grid tray and the solar images formed by the three lenses on the front grid tray are shown in the image plane for a pointing offset of 12 arcseconds from Sun center.

Although the aspect solution itself is independent of twist, the internal consistency of the three independent solutions possible with the built-in redundancy provides a continuous, highly sensitive measure of the relative twist of the upper and lower grid trays during flight. The SAS aspect requirement of 1.5 arcsec corresponds to a sensitivity to relative twist of 0.4 arcmin. During prelaunch coalignment tests, this SAS twist measurement is calibrated against that provided by the TMS discussed above.

Roll Angle System (RAS). For image reconstruction on the ground (no impact on real-time spacecraft operations), knowledge of relative roll is required at all times to 3 arcmin (3σ). Since all sources of torque on the spacecraft are weak, the required information can be obtained with a star scanner that samples the roll orientation at least once per rotation. Interpolation between measurements allows the roll orientation to be determined at intermediate times with the required accuracy.

The RAS (Fig. D-11M) consists of a 2048-element linear photodiode array and electronics (nearly identical to those of the SAS) behind an f/1.0, 50-mm lens. A sunshade limits the FOV so that a 30° band is swept out across the sky orthogonal to the spin axis. As the spacecraft rotates, each detected star generates a brief spike in the output of one or two pixels, whose timing defines the roll orientation. For +2 magnitude stars, the detection signal-to-noise is 15:1. Allowing for Earth occultation and the recovery time from anticipated Earthshine saturation, at least one (and typically seven) such star(s) will be detected each rotation throughout the mission. Measurements of only one star, averaged over a minute, allow the roll angle to be determined to 2.7 arcmin (3σ).

D.2.a.2. Spectrometer

The spectrometer consists of the GeDs, front-end electronics, the cryostat, and cryocooler (Fig. D-11N). We emphasize here that **all aspects of the spectrometer have already been developed.**

Germanium detectors cover the entire hard X-ray to γ-ray line energy range (up to ~20 MeV) with the highest spectral resolution of any detectors (Fig. D-11J). They have been flown on the HEAO-3, Mars Observer, and, most recently, Wind spacecraft (UCB designed/fabricated GeD). Internally segmented GeDs appropriate for HESSI were developed by UCB (Luke 1984), and since 1988 over twenty have been successfully flown on HEXAGONE, HIREGS, and other balloon payloads (Smith *et al.* 1993, 1995; Pelling *et al.* 1992, Feffer *et al.* 1993). These have proven to be very robust; the first ones fabricated and flown are still operating.

The HESSI GeD design provides **wide energy coverage, from ~3 keV soft X-rays to ~20 MeV γ-rays with a single mechanically robust detector**. The largest, readily available, hyperpure (n-type) coaxial Ge material (~7.1-cm diam × 8.5-cm long) will be used. The inner electrode is segmented into three contacts that collect charge from three electrically independent detector segments, defined by the electric field pattern (Fig. D-11R). This provides the equivalent of a ~1-cm thick planar GeD in front of a thick ~7-cm coaxial GeD, plus a bottom <~0.5-cm "guard-ring".

The top and curved outer surfaces are implanted with a thin (~0.3-μm) boron layer to provide a surface transparent down to ~3 keV X-rays. The front segment's closed-end "pancake" configuration is electrically identical (with the same low capacitance) to a commercial ORTEC "LO-AX" GeD. Together with an advanced FET and state-of-the-art electronics, this front segment will easily achieve the 3 keV energy threshold of a LO-AX GeD. Thus, **a separate detector (and its electronics, etc.) is not required for 3-20 keV measurements.**

A window of 20 mils rolled foil beryllium in the cryostat (similar to HEXAGONE) covers the central ~0.2-cm^2 of each GeD with the rest covered by 30 mils aluminum (Fig. D-11S), so that low energy photons are absorbed in the high electric field region over the center contact for optimal charge collection. This window allows for **observations of the iron line complex and thermal continuum down to 3 keV with ~0.5 keV FWHM resolution.**

The front segment thickness is chosen to stop photons up to ~150 keV, where photoelectric absorption dominates, while minimizing the active volume for background. Front-incident photons that Compton-scatter, and background photons or particles entering from the rear, are rejected by anticoincidence with the rear segment; a passive, graded-Z (Pb, Cu, Sn) ring around the front segment absorbs hard X-rays incident from the side, to provide **the unusually low background of a phoswich-type scintillation detector (Fig. D-4).**

Photons with energies from ~150 keV to ~20 MeV, including all nuclear γ-ray lines, stop primarily in the thick rear segment alone, with smaller fractions stopping in the front segment, depositing energy in both the front and rear segments, or in two or more GeDs. All these modes contribute to the total photopeak efficiency (Fig. D-11G).

The intense 3-150 keV X-ray fluxes that usually accompany large γ-ray line flares are absorbed by the front segment, so **the rear segment will always count at moderate rates. This is essential for γ-ray line measurements with optimal spectral resolution and high throughput.**

Photons >~20 keV from non-solar sources can penetrate the thin aluminum cryostat wall from the side and be detected by the GeD rear segments.

Contamination of the intrinsic (flat rear) surface, leading to increased surface leakage current and noise, is the most common failure mode for GeDs. For planar GeDs and silicon detectors, guard rings have long been used to isolate and drain off the leakage current of the intrinsic surfaces. Two years ago, we (UCB) developed the first guard-ring coaxial GeDs, using our segmentation technique to divide the internal electrode <~0.5 cm above the intrinsic (flat) rear surface (Fig. D-11R). Tests with a prototype coaxial guard ring GeD showed no degradation for surface leakage currents of one nanoamp (~ten times higher than usable for non-guard-ring GeDs), and only a few hundred eV broadening in resolution for currents of 10 nanoamps. **This increased resistance to contamination, by a factor of ~10^2, allows the use of a single vacuum enclosure for all 9 GeDs** instead of the more complex and expensive hermetic encapsulation of individual detectors.

Radiation Damage Effects. Reverse electrode (n-type) coaxial GeDs were chosen because of their relative immunity to radiation damage. In the past few years, UCB has conducted extensive studies which show that radiation damage is significantly lowered by maintaining the GeDs at <~75 K instead of the more normal >~85 K, and avoiding warmups above ~85 K and/or high voltage cycling (R. Pehl, private comm.). The cryostat/cooler is designed with large margins (Fig. D-8) to maintain GeD temperatures well below 75 K. The High Voltage Power Supplies (HVPS) are on continuously after turn-on.

In two years near solar maximum, the HESSI 600 km circular, 38° inclination orbit results in a fluence of ~1.5×10^9 cm^{-2} of >30 MeV protons at the GeDs, well below the >~3×10^9 cm^{-2} threshold for significant resolution degradation at 75 K. Thus, neither shielding nor detector annealing (which can reverse the radiation damage effects but entails risk and complexity) is required.

GeD modules and Cryostat. The GeDs are mounted in a module (Fig. D-11S) identical to that for the HEXAGONE and HIREGS GeDs, which have survived many balloon flights and recoveries. The GeD in the module has been successfully vibration-tested and is fully capable of surviving a SELVS II launch.

The GeD modules are mounted on an aluminum coldplate, essentially identical to that for HIREGS. A thin IR radiation/contamination shield encloses and isolates the GeDs. A simple labyrinth seal prevents contamination inside the shield from reaching unacceptable levels over the life of the mission. The shielded GeD assembly is surrounded by a thermal blanket to attenuate the parasitic thermal load on the coldplate. The input FETs are mounted on the module close to the GeD for noise immunity, but thermally isolated to provide operating temperatures of ~120-200K (not critical), as in HEXAGONE and HIREGS.

The shield and coldplate are supported inside the cryostat vacuum shell by low conductivity thermal mounts. The cryostat's curved side wall are ribbed thin-wall aluminum near the GeDs to provide ~20 keV threshold for X-ray/γ-rays incident on the side. The GeDs are kept cold during most ground operations by a liquid nitrogen (LN_2) feed.

Cryocooler. The GeDs are cooled on-orbit by a single electro-mechanical cryocooler. Recently, under contract to NASA/GSFC, Sunpower Inc. has developed an inexpensive single stage, integral (counterbalanced) Stirling cycle cooler which can provide up to 4W of cooling at 77 K, with an input of 100W. This M77 cryocooler has been designed for operational lifetimes greater than 50,000 hours, using a gas bearing/flexure system to prevent contact of moving parts. In extensive studies over the past two years at GSFC, M77 coolers have been vibrated to the GEVS mandated 14.1 Grms, run under thermal vacuum conditions from -25C to +30C, and life-tested already (continuing) for ~>10,000 hrs. Monitoring during these tests showed no

internal contamination of the working gas. Units already tested at GSFC are fully qualified for flight, and will be used for HESSI.

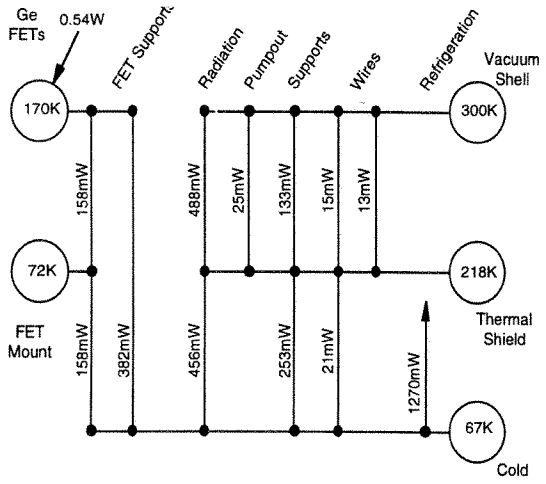

Figure D-8. Heat map derived from a detailed cryostat thermal model.

A detailed thermal model of the cryostat (Fig. D-8), taking into account the FETs, wiring, MLI blankets, support structure, etc., shows that a **single Sunpower cooler will cool the GeDs to 67 K with ~60 W of power, well below the 75 K required.**

Recently, with NASA SR&T funding we (UCB and GSFC) have conducted tests for noise in the GeDs due to microphonics and electrical pickup from the Sunpower cooler. A coaxial GeD in the standard UCB module was mounted on a coldplate connected with a flexible thermal "S-link" to the cold tip of the cooler (the configuration for HESSI). The cooler was run open-loop, without active vibration damping in the tests. **Microphonic and electrical pick-up noise was found to be negligible**, with no significant (<0.1 keV) difference in the GeD energy resolution or noise background with the Sunpower on or off.

The cryocooler electronics provides autonomous startup and shutdown, efficient DC-AC power, and temperature/piston stroke control. These will be packaged separately and mounted near the mechanical cooler.

D.2.a.3. Instrument Electronics

Each GeD is biased at between 4 and 5 kV by a separate adjustable HVPS (developed at UCB for FAST/SMEX and HIREGS). Photons interacting in a GeD generate charge pulses, which are collected and amplified by a transistor-reset Charge Sensitive Amplifier (CSA) (developed by UCB for HIREX) (Fig. D-9) to provide the best resolution and high-count rate performance, and to avoid problems associated with pole-zero cancellation. The FET is an advanced 4-terminal type (developed for UCB and baselined for the ESA INTEGRAL mission) with 3-4 times the gain and half the capacitance of available commercial units.

The CSA signal from the GeD **front segment** goes to two parallel signal processing chains (Fig. D-9). The high resolution "slow" chain consists of a 9-pole quasi-trapezoidal filter amplifier with a peaking time of 4 μsec (developed by UCB), a peak stretcher, and a 16-bit successive approximation ADC (flown on HIREGS). To maintain optimum resolution at high energies >~1 MeV, quasi-trapezoidal filtering is needed to compensate for ballistic deficit effects of the charge collection in large GeDs. The upper 13 bits of the ADC provide 8192 channels of spectral measurements from ~3 keV to 2.7 MeV with ~0.33 keV/channel at rates up to 50,000 c/s.

The high rate "fast" chain (developed for HIREGS) consists of a delay-line shaper generating a triangular pulse of 0.5 μs duration (count rate capability >500,000 c/s), which is sent to a 4-channel stacked discriminator ADC. When the slow chain saturates (Fig. D-5), the accumulated output of these four channels will be sampled at a rate of 16 kHz to provide broad-band ($\Delta E/E \approx 1$) imaging. The fast channel LLD signal is used to detect front-rear and GeD-GeD coincidences, and for pulse pileup rejection.

The GeD **rear segment** has two amplifiers in the slow chain, a normal and a low gain (Fig. D-9), as in HIREGS. The ULD at 2.7 MeV switches the 16-bit ADC to the low gain amp to provide ~2.4 keV/channel up to 20 MeV.

Data formatting follows that for HIREGS. For each detected photon, 14-bits of energy and time of arrival (to 60 μs) are encoded together with detector identification and coincidence flags into a 24-bit event word. This word is latched and a flag raised to signal the formatter card, (based on a FAST design) which simultaneously transfers and formats event data into CCSDS frames. These are sent to the spacecraft mass memory system.

Data Storage. Normally every photon is stored and then sent down. If an extended extremely active period occurs, the main limitation is the orbit-averaged downlink rate.

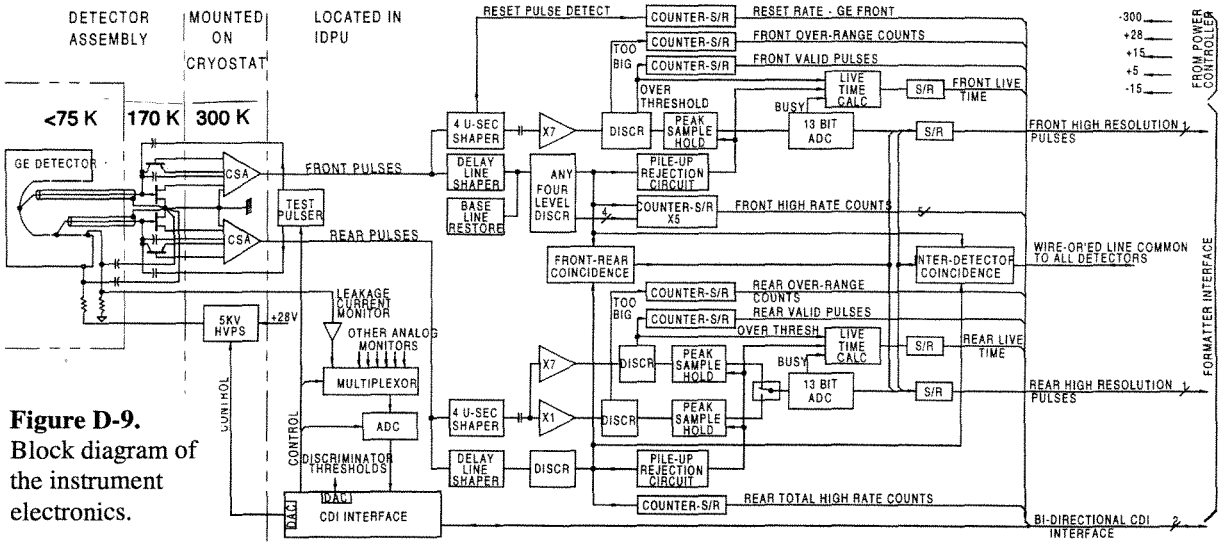

Figure D-9. Block diagram of the instrument electronics.

The GeD rear segments' event rate is always low enough to be stored. When the memory approaches full, the GeD front segments are subsampled by collecting events for an integral number of half-spins for full angular coverage to produce an image, and then not sampling until the input rate matches the expected downlink rate. This method keeps the mass memory from overflowing, with minimum loss of imaging and no loss in γ-ray spectroscopy. Of course, a second ground station could be used to dump the data more rapidly if needed.

D.2.a.4. Calibration and Test

The GeDs are calibrated with a set of radioactive sources ranging from soft X-rays to ~2.6 MeV. Energies up to 15 MeV are obtained using neutron-γ sources. After integration of the Spectrometer, measurements with radioactive sources are made over a range of energies and angles to calibrate a detailed GEANT Monte Carlo model of the Spectrometer with the precise geometry and all materials, as was done for HIREGS and HEXAGONE. This model provides a detailed instrument response for data analysis.

After the Imaging System and Spectrometer have been independently integrated into the spacecraft, radioactive sources are again used to measure total transmission through the grid pairs, and confirm the GeD calibrations.

A calibration pulse generator injects a precisely generated charge pulse into the CSA at ~0.3 Hz for GeD electronics calibration and monitoring. During test mode, this pulser provides a precisely timed pattern of pulses to mimic imaging. These test images are used to check the entire electronics chain, onboard software, and imaging software on the ground.

A final test will be conducted prior to launch to provide end-to-end verification of the performance by determining the modulation amplitude provided by each grid pair in response to a moving X-ray source. For this test, a small gold-foil `gridlet' will be used to define the geometry of an ~100-microcurie source of X-rays (e.g., ^{109}Cd). For suitable distances from the front grids (typically 1–2 m), the gridlet geometry is selected so that PC-controlled motion of the gridlet/source assembly produces strong and calculable modulation in the transmitted photon flux through each grid pair in turn. Data on the X-rays detected with the germanium detectors are recorded and pass through the complete flight data system. The measured modulation as compared to the expected modulation for each grid pair gives an accurate indication of overall performance of the Imaging System.

In-flight, systematic studies of many solar bursts can provide excellent self-calibration, as shown by Yohkoh HXT, and separating out the pulsed emission from the Crab provides a point-source calibration. Ge background lines provide excellent absolute gain calibration.

D.2.b.Mission

The requirements imposed by HESSI on the spacecraft (Table F-2) can be met by a simple Sun-pointed, spin-stabilized spacecraft. The instrument field of view (>~1°) is much larger than the Sun (0.5°) so spacecraft pointing is relaxed and can be automated. The

instrument is on continuously. All of the photon data for the largest flare can be stored in the spacecraft memory and downlinked in <~48 hours, so flare data will rarely, if ever, be lost. Consequently, HESSI is planned for an automated store-and-dump operation, and normally no real-time access is required.

The 600 km circular, 38° inclination orbit can be provided by a standard SELVS II launch. A single LEO-T ground station at UCB provides the required data downlink rate (~1 Gbyte/day), and minimizes tracking, data transmission, and operation costs while allowing the involvement of many students (as in EUVE and FAST). Both the instrument and spacecraft are designed to operate autonomously for weeks at a time, so a single-shift, 5-day-a-week staffing is sufficient.

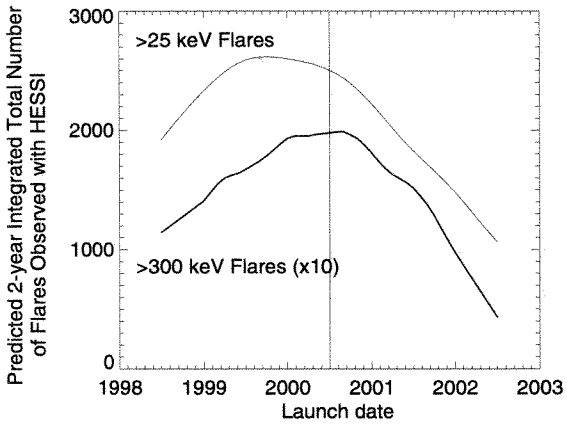

Figure D-10. The predicted **2-year integrated total number** of flares, above 25 keV and above 300 keV, versus launch date (July 2000 planned) (based on HXRBS, BATSE, and Phebus observations).

Launch Date. Figure D-10 shows the predictions of the **integrated total number** of solar hard (>20 keV) X-ray and gamma-ray (>300 keV) flares occurring in a **two-year nominal HESSI mission,** based on the observations of the previous two cycles and the mean period for the last seven cycles of 10.5 years. Even with the uncertainty of ±1 year in the predictions, a HESSI launch in mid 2000 as the first of the two SMEX missions selected by this AO, would be ideal. A launch in 2001 would still be acceptable.

D.2.c. Data Analysis and Archiving

HESSI differs from many imagers in that, instead of transmitting a preselected subset of images, **the telemetry includes all of the information about each detected photon**. Thus, the data analyst can make tradeoffs among time resolution, spectral range and resolution, spatial resolution, image quality, etc., on the ground. These decisions can be made on a case-by-case basis to match the unique characteristics of the event under study and the relevant scientific objective. A key driver of our data analysis approach is the preservation of this flexibility so as to extract the maximum scientific return from the observations. This means that **all detailed scientific analysis will use the same primary database with the most current calibration information**.

In implementing this approach for HESSI data reduction and analysis, we plan for: 1) the complete data output of the HESSI mission to be made available promptly to the scientific community, without restriction; and 2) a fully documented analysis package, supported by a range of platforms, to be available to the scientific community, with the same toolbox of software used by the PI team. A promptly-generated catalog of summary data products will be distributed with the HESSI data base, to serve as a multi-parameter index and overview of the data base and to provide data products to users not requiring custom analyses. Table D-4 lists the specific data products from this effort and the responsible team members.

Table D-4. Data Products

Data Product	Responsible Individual
Primary data base	Smith
Flare list	Schwartz
Flare light curves	Schwartz
Imaging calibration	Hurford
Reconstructed images	Hurford
Spectroscopy calibration	Slassi
X-ray spectra	Schwartz
Gamma-ray spectra	Smith
Complementary data	Zarro
Software distribution /documentation	Tolbert

A Yohkoh SXT Image

B Model Flare

10 arcsec

C

Telescope Demonstration Unit/GSFC
1.7 m long, 45 cm diameter

Test Fine Grids

D

Gold Mask/JPL
34 micron pitch, 25 micron thick, 60 mm diameter

E

Tungsten Grid/Delft
96 micron pitch, 3 mm thick 130 mm square

Enlarged X-Ray Images taken at the X-Ray Facility/GSFC

F Grid Parameters

Grid No.	Resolution (arcsec)	Pitch (mm)	Slit Width (mm)	Slat Width (mm)	Thickness (mm)	FOV (degrees)	Fabrication Technique	Slat Material
1	2.3	0.034	0.017	0.017	0.055	17	Etching	Gold
2	4.0	0.059	0.029	0.029	0.055	28	Etching	Gold
3	7.0	0.102	0.052	0.050	3.0	1.0	Stacking	Tungsten
4	12.1	0.177	0.106	0.071	3.0	2.0	Stacking	Tungsten
5	21.0	0.309	0.184	0.122	3.0	3.5	Stacking	Tungsten
6	36.4	0.530	0.318	0.212	20	0.9	Stacking	Tungsten
7	63.1	0.918	0.551	0.367	3	10	Stacking	Tungsten
8	109.3	1.590	0.954	0.636	3	18	Stacking	Tungsten
9	189.4	2.754	1.653	1.102	30	3.2	Stacking	Tungsten

G Instrument Sensitivity

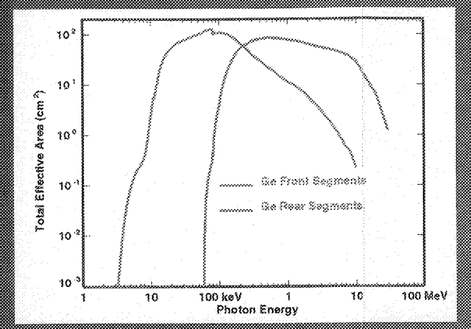

H Instrument Characteristics

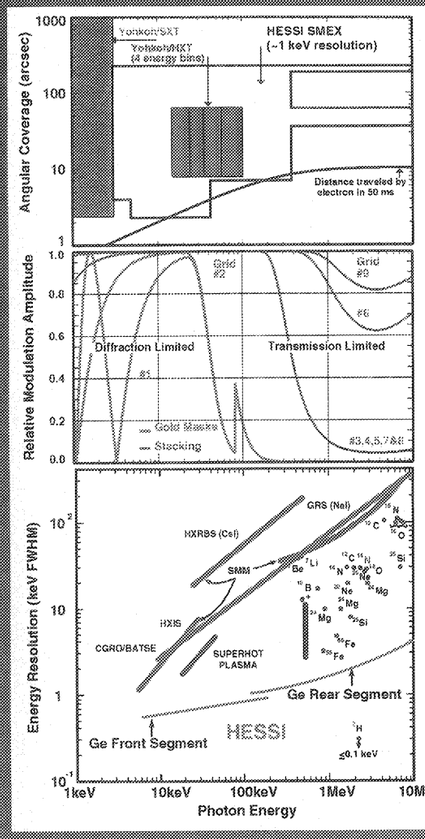

I

J

X-ray and Gamma-ray Imaging Spectroscopy

Imaging

• Angular Resolution (Figure F&H)	2.3 arcsec to 35 keV 7 arcsec to 400 keV 36 arcsec above 1 MeV
• Angular Coverage	2.3 - 189 arcsec (see Figure F&H)
• Field of View	Full Sun
• Temporal Resolution	Tens of ms for basic image, 2 s for detailed image
• Technique	Fourier-transform imaging with rotating modulation collimators
• Grids	2 gold masks, 7 tungsten grids
• Aspect System	SAS to determine direction to Sun-center to <1.5 arcsec RAS to determine roll angle to <3 arcmin

Spectroscopy

• Energy Range	3 keV to 20 MeV
• Energy Resolution (FWHM) (Figure J)	0.5 keV to 30 keV increasing to 2 keV at 1 MeV 5 keV at 20 MeV
• Detectors	Nine germanium detectors each with two segments plus guard ring
• Dimensions	
- Diameter	7.1 cm
- Thickness	Front segment 1 cm Rear segment 7 cm Guard ring 0.5 cm
• Temperature	75K
• Cryosat	Aluminum with contamination barrier around Ge detectors
• Cryocooler	Sun Power
• Cooling Power	Up to 4 watts at 75K

Overall Characteristics

• Total Instrument Weight	120 kg
• Power	110 watts
• Telemetry	Up to 11 Gbits/day

Special Requirements

• Orbit Altitude	600 km, >3-year life
Inclination	38°
• Launch Date	July 2000 planned, as late as Dec. 2001 acceptable
• Operational Lifetime	2 years, 3rd year highly desirable

Spin Axis (to Sun Center within 0.2 degree)

Spin Rate 12-20 RPM

Solar Aspect System (SAS) Lens 4 cm dia. (1 of 3)

Metering Structure 1.5 m long x 45 cm dia.

Flexure Mount to Spacecraft (1 of 3)

Forward Grid 90 mm dia. area (1 of 9)

Rear Grid (1 of 9)

SAS Linear Diode Array (1 of 3)

K Imaging System

M Roll Angle System (RAS)

Cryostat

Germanium Detector (1 of 9)

Thin Aluminum Window, Beryllium Over Central Area (1 of 9)

Time-Tagged Detector Counts

Sunpower Cooler

N Spectrometer

L Prelaunch Twist Monitoring System (TMS)

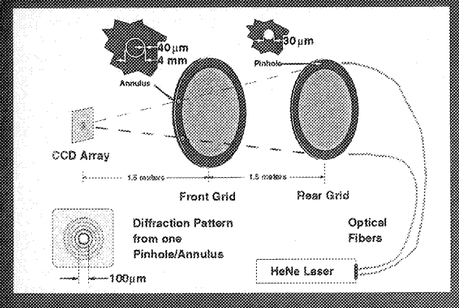

Q Sunpower M77 Stirling-Cycle Cooler

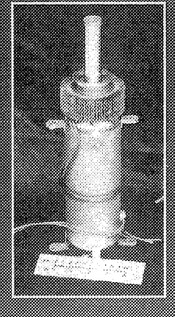

Germanium Detector

R

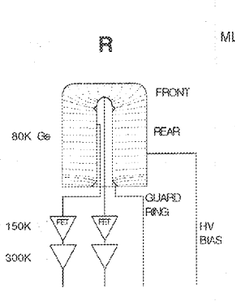

S

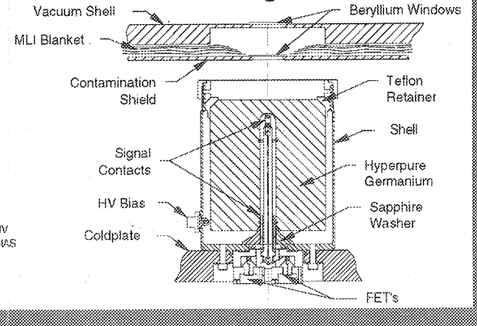

O Count Rate Produced by Model Flare in Each Detector for One Rotation

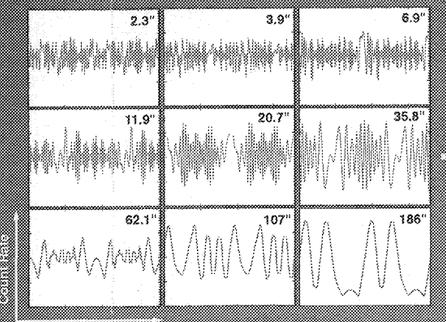

P Reconstructed Image

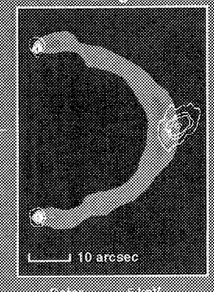

T HIREGS Germanium Detectors and Detector Components

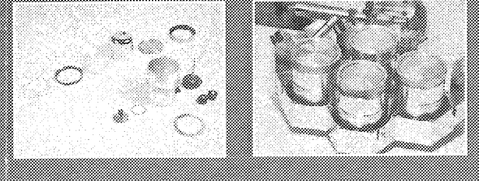

Figure D-11. HESSI Instrument Foldout Sheet

Data Flow and Distribution. The data flow will follow the FAST model that was designed to minimize interfaces and the production of extensive secondary data bases. Data will be telemetered directly from the spacecraft to the MOC/SOC at UCB, where the raw telemetry files will be reformatted into the primary data base. This includes the following principal elements: time-tagged photons, SAS and RAS data, and housekeeping data. Health, safety, and status are confirmed using automated algorithms at this stage. As with FAST, to ensure prompt preparation, the primary data base is generated without routine operator intervention and with no value added except for the addition of "catalog" information. This will include pointers to make the primary data base appear as a sequence of time-ordered, non-duplicated, and quality-flagged data, a summary of spacecraft/instrument status, detector rates above representative energy thresholds, and orbital averages of full-resolution spectra.

For solar events, sets of representative images and spatially integrated spectra will be generated using robust algorithms for inclusion in the catalog. The primary data base and catalog will be made available by network access using a CD-ROM jukebox, and will be shipped to GSFC and ETH on CD-ROMs daily.

At GSFC, the HESSI solar data analysis, distribution, and archiving tasks will be conducted under the auspices of the Solar Data Analysis Center (SDAC). We will take full advantage of the SDAC facilities and experienced personnel developed through the coordinated analysis of data from SMM, Yohkoh, CGRO, and SOHO. In addition to HESSI data, the SDAC will also maintain a database of other relevant spacecraft and ground-based observations.

Table D-5. Data Timeline

Process	Time Required
Data telemetered to UCB	0-48 hrs
Reformat primary data base and generate catalog	≤3 hrs
Generate CDs and ship to GSFC and ETH. Data on line at UCB	≤24 hrs
Data products to NSSDC	≤2 months

A detailed data time line is given in Table D-5. The primary data base and the quick-look data products will be available on line, typically within 24 hours of receipt at UCB. All data products, including the latest analysis software and calibration data, will be shipped to the NSSDC on high-density magnetic tape for archiving within 2 months of real time.

Software Development. The overall HESSI ground software development task can be divided into three areas:

1. Software for prelaunch system-level testing and post-launch operations. Its purpose is primarily command generation, status display, and generation of the primary data base. This software will be developed at UCB based on FAST.
2. Prelaunch software associated with subsystem testing and calibration, developed by the group responsible for the corresponding subsystem.
3. Post-launch analysis software will be coordinated at GSFC, where careful attention will be paid to optimizing user and data interfaces across the different elements.

A software toolbox will be developed to carry out all aspects of the data analysis including the generation of the data products listed in Table D-4. For the most "interesting" computational task, namely image formation from the list of photons, there are several options, all of which have been developed or demonstrated. Each technique has its advantages, with the optimum choice in any situation depending on such issues as photon statistics, computing time restrictions, and map parameters. These techniques include direct Fourier inversion, back projection, maximum entropy, pixon methods, and model fitting.

We have allocated substantial resources to the software development effort to ensure that the data analysis tools will be fully debugged, documented, and tested prior to launch. Our language of choice is IDL. It is easily maintained, well suited to rapid development, can operate seamlessly on many different platforms, and is widely used throughout the solar and astrophysical communities (e.g., Yohkoh and CGRO), allowing us to take advantage of the significant investment in a large body of pre-existing software.

D.2.d Science Team Roles and Responsibilities

The capabilities and experience of Science Team members are given in Appendix I-1.

Professor **Robert Lin** at UCB will lead the Science Team as PI and have overall responsibility for the HESSI mission. Dr. **Brian Dennis** is the lead Co-I in charge of the overall GSFC effort. Professor Lin and Dr. Dennis were Chairman and Study Scientist respectively for NASA's HESP and HESI (precursors to HESSI) Science Study Team. Dr. **Alex Zehnder** is the lead Co-I in charge of the PSI hardware and data analysis effort. No NASA funding is required for the PSI (Switzerland) effort. Co-I **Gordon Hurford** will be the Imager Scientist in charge of Imaging system design and test, and image reconstruction software. UCB Associate Scientist Dr. **David Smith** will be the Spectrometer Scientist, with responsibility for overall Spectrometer development, testing, and γ-ray spectral analysis software.

At **UCB**, Co-I Mr. **Norm Madden** will lead the GeD and front end electronics development. Associate Scientist Dr. **Said Slassi** will lead the Spectrometer calibration, modeling and software effort. Associate Scientist Dr. **James McTiernan** will be the scientist supervising the MOC/SOC operations and participating in the science software effort. Associate Scientist Dr. **George Fisher** will lead the UCB theory and modeling effort. Associate Scientist Dr. **Isabel Hawkins** will lead the UCB Education Outreach effort and coordinate it with her Sun-Earth Connection Education/ Outreach program. All of them will participate in the UCB data analysis effort.

At **GSFC**, Co-I Dr. **Carol Crannell** will lead GSFC's Education/Outreach effort. Co-I Dr. **Reuven Ramaty** will lead the theory and modeling effort for γ-ray spectroscopy and Co-I Dr. **Gordon Holman** for flare energy release and particle acceleration. Co-I Dr. **Tycho von Rosenvinge** will be in charge of ACE/HESSI joint data analysis. Associate Scientist Dr. **Larry Orwig** will lead the grid characterization effort. Associate Scientist Dr. **Richard Schwartz** will lead the X-ray spectral analysis effort. Associate Scientist Dr. **Dominic Zarro** will be in charge of the complementary data. All of them will participate in the GSFC data analysis effort.

At the University of Maryland, Associate Scientists Dr. **Edward Schmahl** and Dr. **Markus Aschwanden** will provide imaging and timing analysis software respectively. Co-I Professor **Richard Canfield** of Montana State University will be the Ground-based Observations Coordinator. Co-I Dr. **Hugh Hudson** will be in charge of white light image alignment software and also participate in analysis of X-ray images. At U. Alabama Huntsville, Co-I Professor **Gordon Emslie** will provide theory and modeling of particle acceleration, transport, and loss processes in flares. Co-I Professor **Frank van Beek** at Delft will provide the stacked grids and mounts, and consultation on fine mechanical engineering.

The following Co-Is do not require NASA funding. Co-I Dr. **Pat Bornmann** at NOAA will lead the GOES/HESSI data analysis and studies related to LSEP event prediction. Co-I Professor **Arnold Benz** will head up the High Energy Data Center in ETH/Zurich for distribution of HESSI data and context ground observations. Co-I Dr. **Nicole Vilmer** will lead the analysis, imaging software, and coordination with radio observation effort at Meudon. Co-I Professor **John Brown** will lead the U. Glasgow theory and modeling effort, concentrating on the X-ray-to-electron inversion problems. At NAOJ, Co-I Professor **Takeo Kosugi** will lead the Japanese effort on hard X-ray imaging analysis, and Co-I Dr. **Shinzo Enome** will concentrate on campaigns with radio observations.

E. EDUCATION, OUTREACH, TECHNOLOGY, AND SMALL DISADVANTAGED BUSINESS PLAN

E.1. Education and Outreach

The educational and public outreach (EPO) efforts will use the energy and enthusiasm of the HESSI Team and the unique aspects of the HESSI mission to excite and educate students, teachers, and the public with this science and technology. Our goals are to provide high-quality research experiences for graduate and undergraduate students, to help teachers provide scientific and technological education to pre-college students, and to contribute toward a technologically and scientifically literate public. We will leverage our limited resources by taking advantage of well-established outreach efforts at UCB and GSFC that use partnerships with science museums and neighboring school districts in disadvantaged urban areas to reach the general public, pre-college students, and teachers. The UCB and GSFC education and outreach efforts will be coordinated by key personnel to ensure the development of complementary materials that can be disseminated through existing structures at both institutions.

As the premier mission in high-energy solar physics, using state-of-the-art techniques for imaging spectroscopy, HESSI will offer outstanding research opportunities for undergraduate and graduate students during all project phases. For the general public and the pre-college community, HESSI will provide exciting and easily appreciated color X-ray movies of solar flares. Such movies will provide spectacular coverage of the biggest events that trigger significant terrestrial effects such as the northern lights, communication blackouts, and power outages. Our educational and public outreach efforts will support teams of teachers, science museum educators, and scientists in the design of classroom materials derived from technological development and scientific research.

UCB Plans. UCB's educational and public outreach efforts will involve graduate and undergraduate students, high school teachers and their students, and the public. At least six undergraduate students and five graduate students will be actively engaged in HESSI research. Also, student employees will staff the HESSI MOC/SOC at UCB. The pre-college program at UCB will be modeled after the highly successful efforts of the EUVE NASA satellite and FAST missions. Dr. Isabel Hawkins from UCB/Center for EUV Astrophysics will lead the UCB EPO. The K-12 program will include in-depth training of a core of lead-teachers from grades 6-12, who work in disadvantaged urban school districts in the Bay Area (San Francisco, Berkeley, and Oakland). **Our collaboration will include Lawrence Muilenburg, a middle school teacher in Walnut Creek; Nellie Levine, Jennifer Fong, and Laurel Rietman from San Francisco public high schools; and Marlene Wilson, Timothy Keys and Emannel Onyeador of Oakland public schools.** These lead-teachers will participate in summer internships at SSL as members of a team that will include museum educators and scientists, working together to develop classroom materials and activities based on HESSI science and engineering. They will then train other teachers in the use of these materials. **The UCB EPO effort will be evaluated by the participation of a graduate student from the UCB School of Education, the Education, Math, Science and Technology Division.**

The UCB effort will build upon a national partnership of science museums established through the Science Education Gateway (SEGWay) program, led by UCB CEA and funded by NASA's High Performance Computing and Communications. The existing national coalitions will provide an effective multiplier of the local HESSI-based education efforts at UCB and at GSFC. The classroom materials developed by teams will be presented on the World Wide Web and on CD-ROMs. They will serve as the basis for training the hundreds of teachers who participate in workshops at each of the SEGWay science museums, including Lawrence Hall of Science, Exploratorium, National Air and Space Museum, and Science Museum of Virginia. Teachers will then be able to use these resources to build or enhance their own classroom materials.

GSFC Plans. At GSFC, several undergraduates will work on all phases of HESSI each summer, and at least one graduate student will pursue a Ph.D. dissertation with HESSI science. The undergraduate research will be augmented with NSF Research Experiences for Undergraduate (REU) funding. This program is in its eighth year with Dr. Crannell as PI and the Laboratory for Astronomy and Solar Physics as an NSF/REU Site. For the pre-college efforts, the principal targeted population is middle-school teachers

and students, where the pipeline problem is most acute. By providing middle school teachers with material and support that they can use to excite their students about mathematics-related disciplines, we can increase the number of students who elect to stay in the math and science track as they approach high school. Part of this effort will be modeled after our ongoing summer teacher program at GSFC, in which we have two or more teachers working with scientists in the Solar Physics Branch for eight weeks each summer on projects such as grid characterization and analysis of solar data.

The teachers will develop educational materials motivated by HESSI science and technology. The scientists and engineers will stay involved with the teachers through visits to their classrooms, guest lectures, and a continuing flow of HESSI information. We have formed partnerships with Harford County Public Schools, Montgomery College Planetarium, and the Maryland Science Center. The points of contact in Harford County are the Southampton Middle School Planetarium and the Aberdeen High School Planetarium, serving 37,000 students in grades K-12. The planetarium teachers have pioneered the development of activity-based classes for middle school students using their planetaria and science data on the WWW as part of the core curriculum with 3000 students and 200 teachers in Southampton and Aberdeen Middle Schools. The Montgomery College Planetarium serves more than 3000 students in grades K through 14 each year with hands-on activities, as well as providing planetarium shows for the general public. The college also sponsors two three-week workshops for 20 high-school and middle-school science teachers per workshop, each summer. One of these workshops will draw on teachers throughout the state of Maryland and the other, on the District of Columbia, a seriously underserved area. These teachers, in turn, will reach a total of 6000 or more students each year. The workshops will provide another forum in which teachers, in partnership with HESSI scientists and engineers, will develop educational materials such as lesson plans, demonstrations, and interactive learning activities.

The Maryland Science Center brings informal science education to people of all ages, with a rich variety of program options for sharing HESSI technology and scientific results with students, teachers, and the public, within the context of the following programs: Camp-In, Career Day, Governor's Academy, Teacher Camp-In, and Exhibit Hall Explainers. Implementing these programs around the time of launch and during intervals of particularly great solar activity will focus attention on the Sun and our understanding of its dynamics. The HESSI team will provide the Maryland Science Center with materials, artifacts, and volunteers to implement these programs. Examples of HESSI materials already in progress include the color movie on HESSI's hard X-ray imaging technology being developed at Caltech, and a lecture demonstration by Co-I van Beek, Delft, on micromachining and kinematic mounts, motivated by our grid technology. We will cooperate with established sources, such as the GSFC Teachers Resource Center, Spacelink operated by MSFC, and various solar home pages, to assure that materials are distributed as widely as possible.

Spectrum Astro. Spectrum participates in a number of community outreach programs involving local schools, disadvantaged children, trade shows, seminars, conferences, trade papers, and magazines. Information in support of NASA programs and technologies is also disseminated on our web page.

We continue to experiment with novel approaches to educational outreach. For example, in 1996 Spectrum sponsored Ross Tucker, an outstanding twelve-year-old student, to attend the launch of the NASA/JPL Mars Pathfinder Spacecraft. As part of this sponsorship, Ross agreed to write an essay on the Mars Pathfinder mission and his launch experience and to make presentations to students at local schools. With the help of Spectrum personnel, Ross put together an excellent presentation and is now visiting schools in the Phoenix area encouraging other young people to share his interest in space science.

We will work with UCB during the course of the program to jointly assess and evaluate beneficial outreach strategies. These strategies will promote public understanding of the objectives and benefits of the HESSI program in specific, and the exploration of space in general.

E.2. New Technology

Several technology items have *already* been developed for HESSI (with NASA funding, of course). They include: (1) fine grids made from high-Z materials by foil

stacking with grid thickness to slat width ratio of ~50:1; (2) segmented and grounded guard-ring coaxial GeDs; (3) advanced FETs; (4) transistor-reset CSAs, (5) low-cost, high-capacity cryocoolers. **No further technological developments are required for the HESSI mission.**

Technology items already developed for HESSI have significant potential for transfer to other NASA missions, the federal government, and the private sector. The transistor-reset CSA circuitry is presently offered by all the major GeD manufacturers in their premium (extra cost) electronic systems. We are considering an offer by a commercial firm (Amptek) to hybridize our CSAs for HESSI in exchange for marketing rights. The advanced FETs are baselined for the European Space Agency INTEGRAL (INTErnational Gamma-Ray Astrophysics Laboratory) mission as part of NASA's involvement. The UCB segmented GeD technology will be transferred to ORTEC since they can provide GeDs on our schedule.

Potential fine grid applications (many have been discussed with commercial entities) include X-ray imaging for high volume baggage inspection, characterization of heavy metal deposits, radioactive waste assessment, medical imaging, comb drive actuators and a micro mass spectrometer.

The Sunpower cryocooler has been baselined for many ground applications as well as a number of sub-orbital and other space experiments.

E.3. Small And Small Disadvantaged Business Contracting

The HESSI team will easily meet the 8% SB and SDB requirements for a SMEX Program.

At UCB, we use the Minority and Women Business Enterprise Directory maintained by the UCB Office of Minority Business Development in selecting subcontractors. In the SMEX FAST project, for example, we assisted an SDB contractor (M-B Systems) to develop the circuit board assembly capability to NASA standards, including ESD control and NHB5300.4 certification thoughout.

At GSFC, center management is very committed to SB and SDB development and maintains an aggressive policy of offering mainstream scientific and technical development opportunities to SBs and SDBs. This enhances their base capabilities and competitive posture for acquiring future related work. GSFC flows down SB and SDB goals of at least 8% each to all contracts with non-SBs in excess of $500k.

The spacecraft provider, Spectrum Astro, is classified as both a small business and Small Disadvantaged Business. At approximately 200 current employees, it will probably remain in the small business category for the duration of the HESSI period of performance. Spectrum's Standard Industrial Classification (SIC) code is 3761. It is a women-owned business with 52% of the company stock controlled by women. Ms. Martha S. Martin is the Chief Executive Officer and Ms. Patricia M. Oleson is both Vice President of Contracts & Finance and Chief Financial Officer. The combination of small and women-owned business classifications meet the requirements of NASA's SDB program.

Since the spacecraft alone represents approximately 21% of the total budget, HESSI will comfortably exceed the SB and SDB goals.

F. MISSION IMPLEMENTATION

F.1.Mission Overview

The HESSI Mission involves a single instrument consisting of an Imaging System, a Spectrometer, and Instrument Electronics, mounted in a simple Sun-pointed, spin-stabilized spacecraft. The instrument and science objectives are summarized in foldout Figure D-11 and the spacecraft in foldout Figure F-1 (end of this section).

HESSI will be launched in mid-2000 on a small-fairing SELVS II vehicle into a 600-km circular, 38° inclination orbit, in a standard configuration with the spacecraft ON and the instrument OFF (detectors warm). Following injection into orbit, the spacecraft will reorient towards the Sun, deploy its solar arrays, and spin up to 15 RPM.

The spacecraft will then transition from course to fine Sun sensor pointing, turn on the SAS and RAS, and position the Sun within the SAS field of view. After confirming SAS functionality, the spacecraft will be directed to use SAS signals, providing a fully-automated closed-loop pointing system referenced to the Imaging Systems' boresight.

Once the operational attitude, orientation and spin rates have been achieved, the instrument electronics and cryocooler will be powered. Using a preprogrammed thermal profile, the cryocooler will cool the spectrometer to operational temperatures within a few days. This will be followed by a brief detector checkout period in which high voltages are turned on before normal operations begin.

In normal operation the GeDs are kept <75 K, GeD high voltage is on, and observations are taken continuously. Because of the large thermal mass of the GeDs the cryocooler can be cycled over time scales of hours if needed. Energy and arrival time of every photon detected, together with instrument SAS and RAS attitude data, are stored in the spacecraft's 2 Gbyte mass memory and then telemetered. Ground data systems will convert these data into X-ray and γ-ray images and spectra.

A LEO-T ground station at UCB is planned for all command and data reception. A Mission/Science Operations Center at UCB will operate the spacecraft and instrument, write the data onto CD-ROMs, and distribute them to the Solar Data Analysis Center (SDAC) at GSFC and the High Energy Data Center (HEDC) in Zurich. The SDAC will archive and distribute both data and analysis software to outside users in the U.S., and provide context observations from other spacecraft and ground instruments. The HEDC will perform the same functions in Europe. A program of ground observations is supported directly by HESSI to provide critical context data.

The Mission Elements are summarized in Table F-1 and discussed below. The spacecraft is described in detail in section F.2 and ground systems in section F.3, and potential risk areas and mitigation in section F.4.

Product Assurance. Product Assurance and Configuration Management will be based on those used successfully on SMEX FAST, SOHO XDL, Wind 3D Plasma, Polar EFI, etc. An overall CM Plan will be developed which incorporates instrument, spacecraft, and ground segment documentation.

Table F-1 Mission Elements

Mission operations scenario:	Continuous observations with data stored on-board and dumped periodically.
Spacecraft pointing requirements:	Spinning spacecraft with spin axis <0.2° from Sun center; 15 rpm spin rate (12-20 rpm acceptable).
Attitude determination:	Instrument SAS & RAS give spin axis attitude to 1.5 arcsec, roll 3 arcmin.
Orbit determination:	NORAD orbit determination accuracy sufficient for both ground station contacts and science data analysis.
Communication requirements:	Required downlink capability to dump 12 Gbits from memory in 48 hours, easily satisfied using a LEO-T at UCB with 3.5 Mbps downlink and 2 kbps uplink.
Mission lifetime:	2 years nominal, 3 years desired.
Launch and/or operational windows:	Launch in mid-2000 planned; by end of 2001 acceptable.
Orbital requirements:	38° inclination, 600 km altitude, circular for ≥3-year lifetime.

Table F-2. Instrument Requirements on Spacecraft

Requirement	Accommodation
Provide instrument orbit average power of 110 W	110 W accommodated with 20% margin
Accommodate instrument mass of 130kg	130 kg accommodated with 13.8% spacecraft growth allowance and 47% launch vehicle contingency
Spin instrument at a rate of 12-20 rpm	S/C spun up and kept at 15 rpm with magnetic torquer bars
Point instrument axis within 0.2° of Sun center for all solar observations	Spacecraft is dynamically balanced before launch. Linear mass drivers to adjust in orbit. Use pitch and yaw error signals from instrument Solar Aspect System in spacecraft ACS.
Store >~ 2 Gbytes of instrument data	2.0 Gbytes of data storage
Downlink >~ 8 Gbits per day instrument data	Average data output of 11 Gbits per day
Front and rear grids must be at the same temperature to within 3° C.	Thermal blankets over telescope plus 9 watts of thermostatically-controlled heater power
>1% transmission of >3 keV solar X-rays through material above detectors	Thermal blankets limited to total of 10 layers of MLI above and below grid trays
Clear optical paths for SAS and RAS	Apertures in thermal blankets above three SAS lenses. Clear side view for RAS
Provide largest possible clear FOV for cosmic source detection	No spacecraft components located around spectrometer
Dump ~ 60 watts of heat from cryocooler	Radiator provided at anti-Sun side of Spacecraft

Launch Date. The required HESSI launch date and useful mission lifetime are determined by the timing of the next solar activity maximum. Predictions based on the last two solar cycles indicate that several thousand hard X-ray flares and of order a hundred γ-ray flares will be detected in a two- or three-year HESSI mission starting in mid-2000 (Figure D-10). Even a launch as late as the end of 2001 or an unusually early solar maximum would not reduce the predicted number of hard X-ray flares below 1500. Thus, the first of the two SMEX missions being selected through this AO, with a launch in mid-2000, would be ideal for HESSI.

Orbit. We propose to launch HESSI into a simple 600 km circular orbit, chosen for >3-year orbit lifetime, inclined at 38° for communication and operation simplicity. While this orbit is higher in radiation than an equatorial orbit, tests of the GeD detectors show that radiation test damage is not a problem for a 2-3 year mission if the GeD are kept at temperatures below 75 K, easily achieved with HESSI cryocooler and cryostat design.

Instrument Accommodation. The HESSI instrument places modest requirements on the design and operation of the spacecraft (Table F-2) so a simple, spin-stabilized spacecraft with extensive use of currently available, space-qualified components and subsystems is adequate.

Ground Based Program. Ground-based observatories are a unique source of the optical and radio data (Table F-3) that are crucial to the successful interpretation of the HESSI data. We have allocated HESSI funds for the necessary upgrading of hardware at these observatories to provide measurements with adequate temporal resolution, dynamic range, and data handling capabilities for comparison with HESSI's observations. For two facilities that lack long-term support, we will provide the minimal support during the mission to ensure the operation of these critical and unique instruments.

Table F-3. HESSI US Ground-based Program

Filter-based vector magnetograms	MSFC, BBSO
Stokes-polarimeter vector magnetograms	NSO/SP, BBSO
Microwave imaging spectroscopy	OVRO
Optical imaging spectroscopy	BBSO, NSO/SP
Millimeter-wave imaging	BIMA
Full-disk images, magnetograms	NSO/SP,/KP, BBSO
High-resolution imaging	BBSO
Multiband imaging	NSO/SP
Microwave and optical patrols	SOON, RSTN

F.2. HESSI Spacecraft

Our guiding philosophy in the design of the HESSI spacecraft is to drive toward firm requirements definition, conservative design margins, utilization of standardized and proven electronic interfaces, minimum parts count, proven designs, operational simplicity, and maximum use of existing plans, procedures, and processes. The HESSI spacecraft, shown in Figure F-1, is consistent with this philosophy and accommodates all of

the HESSI instrument requirements using space-qualified components and approaches. Table F-4 is a summary of the mass and power characteristics of the spacecraft and illustrates our conservative margin approach; we have **designed-in allowances for 15% growth in spacecraft bus mass, 20% in instrument mass, and 20% in power. In addition to these growth allowances, our design incorporates 47% launch vehicle mass contingency.**

Table F-4. Mass and Power Characteristics

Subsystem	Mass (kg)	Orbit avg pwr (W)
Structure & Mechanisms	18	-
Electrical Power	26	-
C&DH	15	35
Telecommunications	6	1
Attitude control	16	7
Thermal	2	3
Cabling	6	-
Balance	5	-
Growth (13.8% Mass, 20% Power)	15	9
Bus	**108**	**55**
Payload	130	110
Spacecraft	**238**	**165**
LV Mass Contingency (47%)	112	
LV Mass Capability	**350**	

Structure & Mechanisms. The primary structure is composed of a single aluminum honeycomb panel and a thrust tube to carry loads from the launch vehicle adapter ring. The open structural design permits thermal radiator area for heat rejection and enables access to spacecraft and instrument components throughout all phases of integration and test to reduce cost and schedule. All spacecraft components are attached to the mid-deck panel allowing the spectrometer to have an unobstructed radial field-of-view. The spectrometer and the imager assembly are structurally independent from one another, allowing separate bolt-on installation - the imager assembly is installed from above the mid-deck and the spectrometer is installed from below.

The mechanism subsystem consists of the mechanisms to support the deployment of four identical solar array wings. A single shaped memory alloy (SMA) actuated release device preloads the wing against the cup and cone snubbers in the stowed configuration. Advantages of the SMA include lower cost, lower mass, higher reliability, negligible shock loads, and the capability of being operated through repeated test cycles allowing protoflight qualification of the actual flight units. HESSI contains no pyrotechnic devices, thereby minimizing safety and range interface concerns.

Spacecraft dynamic balance is critically important to the operation of the instrument, and spacecraft components have been located with considerable attention paid to inertia properties. The result is an efficient, symmetrical, well-balanced spacecraft design that is ideally suited for this spin-stabilized configuration. In addition to the design efforts, the spacecraft will be spin-balanced following final system test, and linear mass drivers will be used on-orbit to do the fine adjustments that may be necessary following deployment of the solar array wings.

Electrical Power. The electrical power subsystem consists of the four silicon-cell solar array wings, a single Common Pressure Vessel (CPV) NiH_2 battery and all spacecraft cabling. Battery charging, power conversion and distribution are performed within the integrated electronics module (IEM) of the Command & Data Handling subsystem. Each solar array wing consists of Al facesheet/Al honeycomb substrate with 2 ohm-cm, front surface passivated silicon cells and produces over 81 Watts at end of life for a total spacecraft power of 325 W. The battery stores power in ten 12 amp-hour CPV cells connected in series to produce 28 ±4V. The IEM hosts the power input/output (PIO) board and the charge control board (CCB). The PIO, developed by Spectrum for Lunar Prospector, provides VME-controlled, 28 ±4 V switched power outputs. The CCB, also developed for Lunar Prospector, uses pulse-width modulated FET switches to control the direct flow of array current to the battery. The cabling approach is based upon Spectrum's MightySat and New Millennium Program (NMP) DS-1 designs.

Command & Data Handling. The Command and Data Handling subsystem is built around the VME-based integrated electronics module (IEM) which contains the 1750A CPU, communications interface board (CIB), payload and attitude control interface (PACI), charge control board (CCB), power input/output (PIO), 2 Gbyte solid state

memory, and 5 spare card slots. The 1750A has been developed by Southwest Research Institute (SWRI) and Spectrum Astro in support of MSTI, MightySat and NMP DS-1 and has been previously flown on MSTI-1, MSTI-2, and MSTI-3.The CIB, PACI, CCB, and the PIO were developed by Spectrum in support of Lunar Prospector, Mars-98 Orbiter and Lander, and NMP DS-1. The solid state memory is supplied by SEAKR based on space-qualified hardware produced for NASA's SSTI program.

Attitude Control System (ACS). The Attitude Control System consists of four coarse Sun sensors, a fine Sun sensor, three torque rods, a magnetometer, two linear mass drivers, and a passive nutation damper. The spacecraft will separate from the launch vehicle in 3-axis mode, deploy the four body-fixed solar array panels, acquire the Sun using four coarse Sun sensors with 4π steradian coverage, spin-up to 15 RPM and perform Sun acquisition to 0.2° using the fine Sun sensor. This Sun-pointing attitude will be maintained throughout the mission using Sun attitude data from the spacecraft fine Sun sensor and the instrument SAS. Spacecraft attitude will be continuously changed to follow the Sun using internally redundant torque rods in combination with magnetic field data from the 3-axis magnetometer. The passive nutation damper is used to damp nutation which can also be actively controlled using the torque rods. The linear mass drivers allow fine control of the spacecraft moments and cross products of inertia in the final deployed configuration ensuring stable, smooth, spin during the entire mission.

Both the instrument and the spacecraft have been designed to operate autonomously for weeks at a time. Following the initial attitude acquisition, even if the Attitude Control subsystem should fail "off", the spacecraft spin axis will remain fixed in inertial space.

Telecommunications. The Telecommunications subsystem consists of a 5-Watt STDN S-band transponder, RF assembly, and two omni antennas and ensures full downlink capability regardless of spacecraft attitude. The downlink rate to the UC Berkeley ground facility is 3.5 Mbits/second with 2.6 dB link margin, using a ground antenna diameter of 5 meters as shown in Table F-5. The data is BPSK coded using CCSDS recommended r=1/2, k=7 concatenation with RS(233,255). This approach results in an average of 11.2 Gbits of data downlinked per day.

Table F-5. Link Margin

Parameter	Value
Carrier Frequency (MHz)	2200 to 2300
Elevation Angle	5° or greater
Transmitter Power (W)	5
Modulation	BPSK or QPSK
Data Rate (Mbps)	3.5
BER	<1 in 10^5
FEC inner code	RS(233,255)
FEC outer code	k=7, r=1/2
Assumed Ground Station	5 m with G/T 16.2 dB/K
Availability	99.99%
Margin at 5 ° Elevation Angle	2.6 dB

Thermal Control. HESSI uses a proven, cold-biased design with flight proven technologies to provide an inherently reliable thermal control architecture. All thermal control components are standard, off-the-shelf hardware. The instrument is thermally isolated from the spacecraft to ensure that spacecraft thermal properties do not affect science operations.

F.3. Ground Systems

The HESSI mission operations scenario (see Figure F-2) is simple and efficient. Both the spacecraft and the instrument are fully autonomous during normal operations. No commands need be sent to the spacecraft for days or even weeks at a time, other than those required to activate the transmitter and dump data during each ground-station pass. Thus, once all spacecraft and instrument functions have been activated and verified after launch, the mission operations scenario consists merely of reading out science data from the onboard memory each orbit and verifying the health and safety of the mission.

We propose to install a single LEO-T ground station at Berkeley for commanding and data reception. LEO-T is a small autonomous station for tracking low Earth orbiting spacecraft. It includes a 5-meter dish, RF electronics, and a CCSDS-compatible front-end processor. It is identical to the station being installed in Puerto Rico for the FUSE mission. HESSI will make 6 passes per day of about 7 to 10 minute duration over the UCB station. A 2.6 dB link margin from HESSI to LEO-T can be maintained at 3.5 Mbps transmit rate, giving a daily downlink data volume of 11 Gbits (Table F-5). The FUSE ground

station can be used as a back-up for HESSI, and the Berkeley ground station can be made available to NASA for other missions.

HESSI will use the Integrated Test and Operations System (ITOS) to satisfy both Integration and Test (I&T) and Mission Operations Center (MOC) requirements (Fig. F-2). ITOS was developed at GSFC as an I&T system for SMEX missions, and was used by the FAST spacecraft for I&T. Later ITOS evolved into a system which satisfies both I&T and MOC needs, and is being used in both capacities by the TRACE mission. ITOS can perform health and safety monitoring, commanding, ground station control, mission planning, and orbit and attitude determination. Using the same system for I&T and MOC greatly reduces costs and schedule risks. Furthermore, UCB personnel are already familiar with ITOS from their FAST experience. The Science Operations Center will be nearly identical to the system developed for FAST at Berkeley. This autonomous system performs instrument monitoring, selected data reduction (with data plots automatically posted to a page on the WWW), and data distribution in the form of CD-ROMs (automatically labeled). The entire system operates with no human intervention. Data will be transferred by CD-ROM to the SDAC data archive at GSFC and the HEDC archive at Zurich from which it can be accessed generally.

Co-locating the ground station, Mission Operations Center, and Science Operations Center at Berkeley eliminates ground communications costs and reduces personnel requirements during operations. The whole system can be operated by two people on a one shift per day basis (plus student help and occasional consulting by subsystem experts). Automated spacecraft and instrument health monitoring at the MOC (an off-site operator is notified in case of a problem) is desirable to minimize possible data loss, but is not required. Mission planning and real-time support is required only during launch and initial orbit acquisition.

F. 4. Potential Risk Areas

The HESSI team has worked diligently to remove schedule, cost, and technical risks from the program and will work with the SMEX office to assess and mitigate potential risk elements. Because essentially all the required development work for the HESSI instrument has already been done, and the spacecraft consists almost entirely of already qualified subsystems, the risks involved for HESSI are minimal, much lower than for the typical SMEX. Below, we discuss specific possible risk areas that have been identified, and possible mitigation.

Schedule. The schedule is tight but we have done all the development work and made the arrangements required to make it clearly achievable. There is 14 to 16 weeks of distrbuted slack for the instrument and spacecraft, respectively, for a July 1, 2000, launch. There is an additional 3 months of contingency to meet the launch requirement of September 2000 for the first SMEX chosen under this AO. Delays will decrease the number of flares detected (Figure D-10) but even a launch at the end of 2001 would still be scientifically acceptable.

Cryocooler. The Sunpower cryocooler is new technology. It has been fully flight-qualified and tested with the GeDs so we are very confident that it will be successful, but it has not flown previously. If significant problems arise, we can go to another flight-qualified cooler (3 others have been tested by UCB and proven compatible with GeDs).

PSI Fabrication of the Imaging System. PSI (Paul Scherrer Institute) has extensive experience with fabrication of space flight hardware and has always delivered successfully. However, we have costed the effort required to duplicate PSI's tasks (given in the budget as PSI contribution) in the U.S., and are confident that they can be done by UCB or a subcontractor for that cost.

Grid Fabrication. Grids #3-9 are being fabricated by Co-I van Beek. The technology is fully developed, but if problems arise these grids can be replaced by the JPL gold foil grids with loss of imaging at high energies (above ~40 keV). This would be an acceptable science fallback. The gold foil grids can also be fabricated by outside vendors as well as JPL.

GeD fabrication. In the very unlikely event that problems arise at ORTEC, the GeDs can be fabricated at UCB with some delay in the schedule (see above), but no other impact.

HESSI Spacecraft Features

Spacecraft System Design

- **Compact spacecraft design**
  - Compatible with SELVS II baseline launch vehicle with small fairing
  - Launch mass of 268 kg includes ample growth allowances and provides an additional 25% launch vehicle mass contingency
  - Well-balanced, symmetrical design
- **Spin-stabilized spacecraft**
  - Increases simplicity
  - Reduces component parts count
  - Reduces failure modes
- **Four solar array design, spin balancing, and linear mass drivers enable accurate tailoring of inertia properties**
- **Extensive use of previously space-qualified components - NO NEW DEVELOPMENT REQUIRED**

Structure & Mechanisms

- **Aluminum honeycomb primary structure panel decreases complexity and integration costs**
- **All aluminum secondary structure**
- **Simple, proven mechanisms**
- **No pyro-activated devices**

Thermal Control

- **Passive, cold-biased system use local radiators**
- **All standard, off-the-shelf thermal components**

Electrical Power

- **Direct energy transfer system with controlled battery charging**
- **Four solar array panels using 2PR Si cells with 30 mil covers provide > 325 W at 2 years**
- **Al facesheet/Al honeycomb substrates**
- **Two (10) cell, 12 A-hr Common Pressure Vessel NiH_2 batteries have over 83% margin**

Flight Software

- **Full and partial on-orbit reprogrammability**
- **High reuse of software developed by Spectrum for Lunar Prospector (another spin-stabilized spacecraft)**

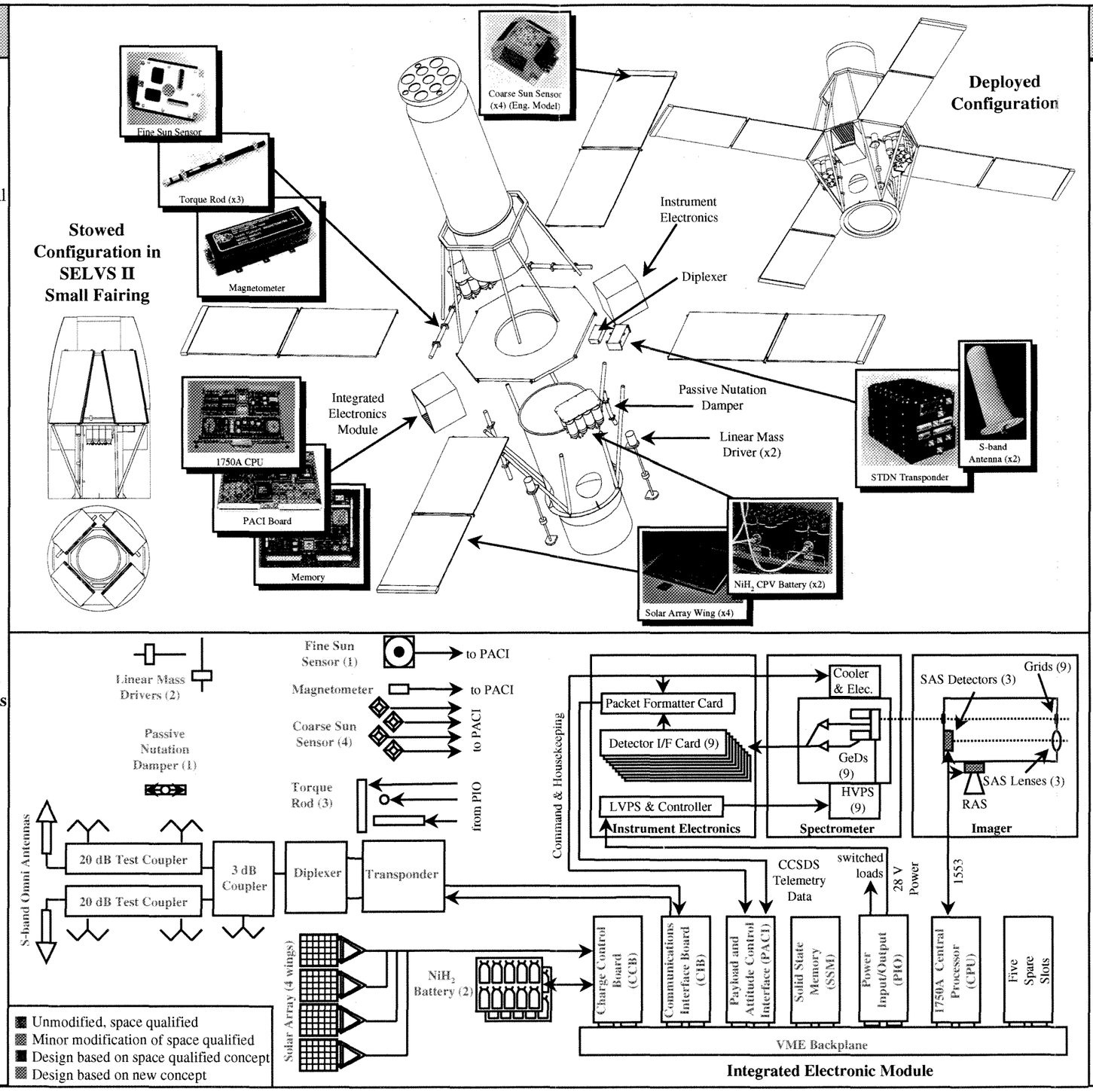

HESSI Spacecraft Features

Attitude Determination and Control

- **Simple, reliable, and robust spin-stabilized attitude control**
- **Passively spin stable with ~10% margin (I_S/I_T)**
  - 25 kg can be added to S/A panels for growth
- **Only basic Sun-pointing ACS needed**
  - ACS safehold and eclipse modes are off
- **Four coarse Sun sensors used during first phase of attitude acquisition to bring spacecraft within fine Sun sensor FOV**
  - Identical to Spectrum's MightySat
  - 4π steradian coverage
  - Provides knowledge to < 2°
- **Fine Sun sensor used during second phase of attitude acquisition to bring spacecraft within instrument's SAS FOV**
  - Similar to Sun sensor on JPL/Spectrum DS-1
  - 32° field-of-view
  - < 0.05° knowledge
  - Back-up to SAS to provide degraded instrument operation
- **Magnetometer used in conjunction with three torque rods provides attitude control**
- **Passive nutation damper for early operations**
  - Torquer-based active damping is possible
  - Only arcsec nutation is induced by ACS
- **Linear mass drivers allow on-orbit adjustment of balance (± 1°) following array deployment**

Command and Data Handling

- **Integrated electronics module contains C&DH and power control electronics to reduce cost and mass**
- **Processing performed by rad hard, high reliability 1750A**
- **2.0 Gbytes of solid state memory**
- **Latch-up immune, total dose tolerant parts**

Telecommunications

- **S-band system with STDN-compatible transponder**
- **Downlink at 3.5 Mbits/s with 2.6 dB link margin**
- **4π steradian coverage with two omni antennas**
- **100% off-the-shelf components provide high heritage, low risk solution**

Figure F-1. The HESSI Spacecraft Design Is Based on Existing, Space-Qualified Designs and Approaches to Give the SMEX Program a High Science Return, Low Risk, High Heritage Option for the Year 2000 Mission

Figure F-2: HESSI I&T AND MISSION OPERATIONS PLAN

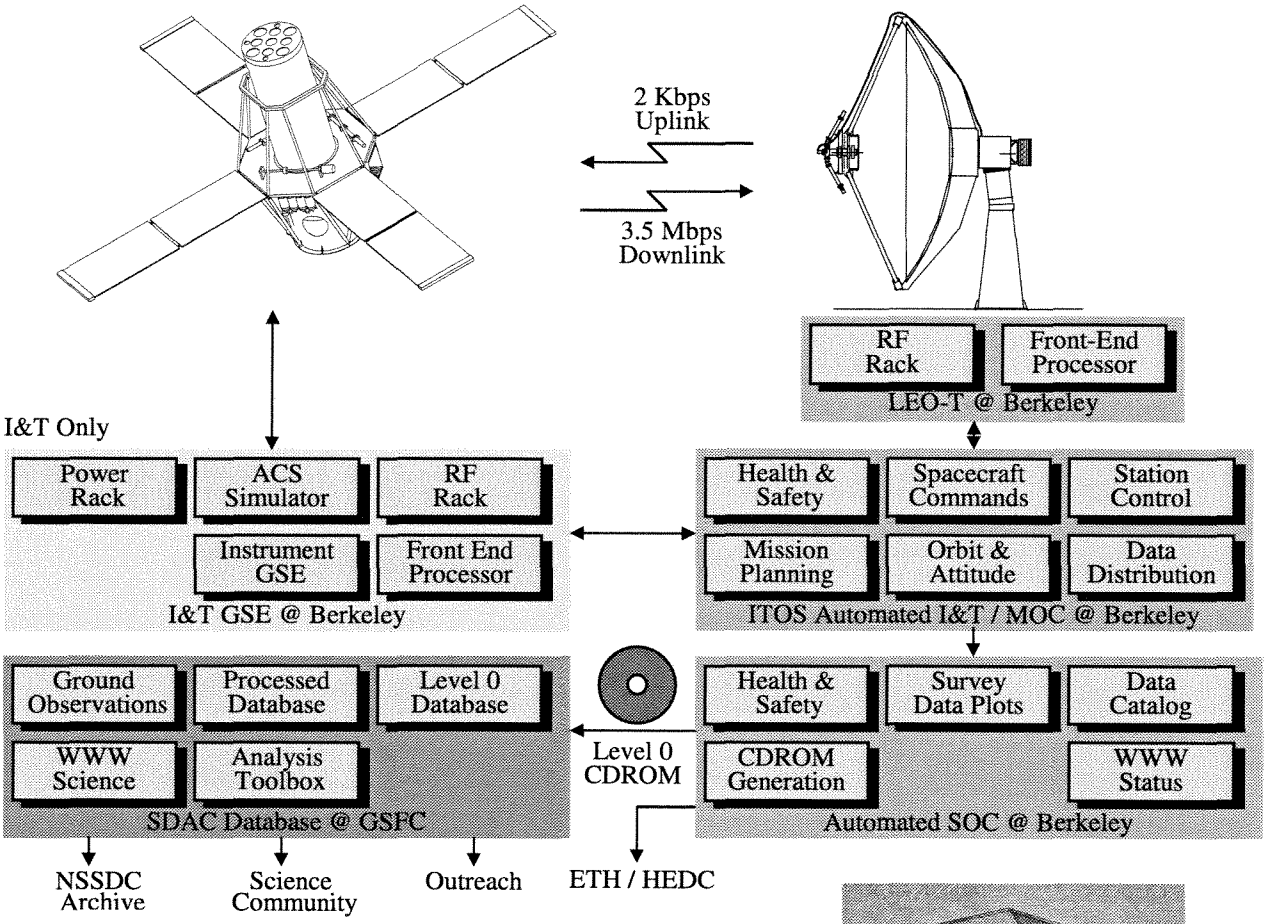

Integration & Test Flow

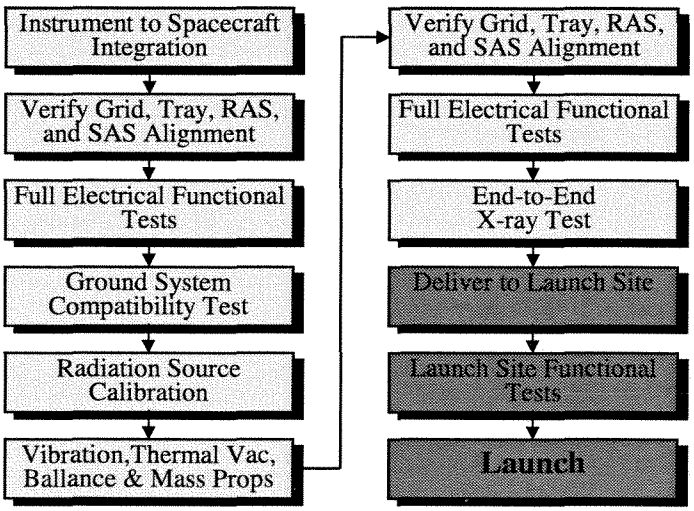

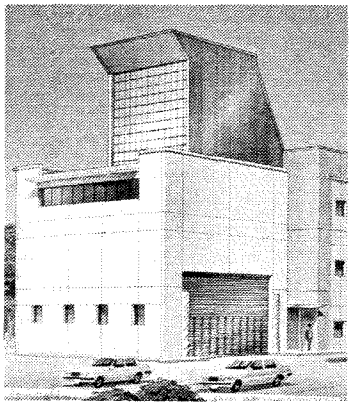

New High-Bay Facility at Berkeley

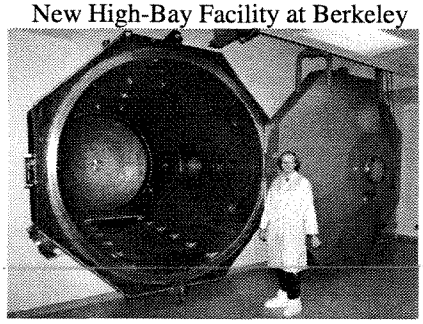

Large (Thermal) Vacuum Tank at Berkeley

G. MANAGEMENT AND SCHEDULE

G.1. Approach

The HESSI project features a committed team of scientists and an industry partner experienced in small spacecraft efforts.

The **Management Organization** (Fig. G-1) will be based on that for the UCB FAST/SMEX. The PI will be the point of contact with the SMEX project HESSI Mission Manager. Reporting directly to the PI will be the Project Manager (PM), Mr. Peter Harvey, who will supervise and coordinate the instrument development at UCB, GSFC, and Paul Scherrer Institute (PSI); the spacecraft development at Spectrum Astro, our industry partner; and the ground system development, integration and test, and mission operations preparation at UCB. Following launch, the PI will direct the Mission/Science Operations at UCB, and lead the overall science analysis effort, with support of the Co-Is, the Education/Outreach and the Ground Observations Coordinators.

Figure G-1 Organization Chart

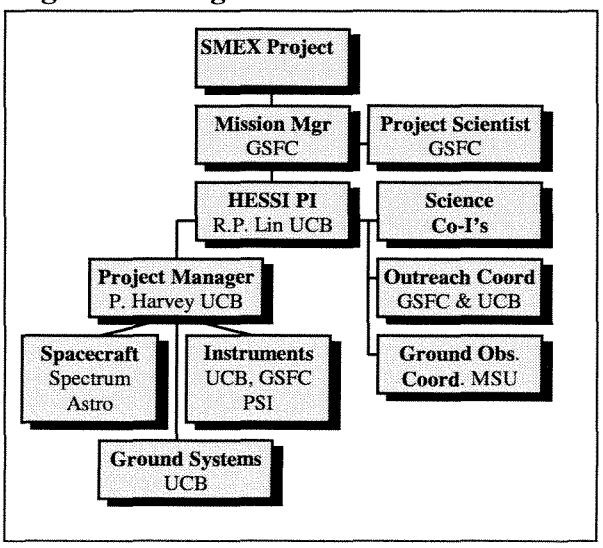

Decision-making process. The PI will delegate to the PM the responsibility and decision-making authority for the day-to-day operation of the project, with particular emphasis on cost and schedule control. The PM will develop an integrated (UCB, GSFC, PSI, Spectrum Astro) cost and performance report, and provide monthly submissions to the PI and the HESSI Mission Manager. Major decisions regarding cost or performance changes during development will be made by the PI in consultation with the PM and lead Co-Is at GSFC and PSI (and the project manager at Spectrum Astro for spacecraft issues).

Teaming arrangements. The HESSI hardware development team consists of UCB, GSFC, PSI, and Spectrum Astro (Table G-1). UCB was designated as the PI institution and developer of the Spectrometer, based on the solar high-energy (HIREGS, HIREX balloon program) and space-flight experiment expertise (see Appendix I) of Professor Robert Lin, and on the capabilities of the UCB Space Sciences Laboratory (FAST, SOHO XDL, Polar EFI, Wind, EUVE, etc.). GSFC, under lead Co-I Dr. Brian Dennis, was designated to lead the grids and cryocooler effort based on their HEIDI balloon program, their grid characterization expertise, and their cryogenics experience on numerous programs. PSI, under lead Co-I Dr. Alex Zehnder, was chosen for the telescope, RAS, and SAS, based on their experience on XMM, EUVITA, and MIR. Spectrum Astro, our industry partner, was chosen to provide the spacecraft, based on their outstanding record in small spacecraft (MSTI 1,2,3; New Millenium DS-1, MightySat), and their flight-qualified subsystems useful for HESSI.

The division of tasks was chosen to take advantage of the strengths of each partner and

Table G-1 Team Member Responsibilities

Team Member	Role	Relevant Experience
UCB	Project Management	FAST, Polar, Wind,
	Spectrometer	HIREGS, TGRS, HEXAGONE
	Instrument Elect.	HIREGS, FAST
	Flight Software	FAST, HIREGS
	Ground Data System	FAST ITOS
	Mission I&T	FAST, Polar, Wind
	Flight Ops	FAST SOC
	Data distribution	FAST SOC
GSFC	Grid Characterization	HEIDI
	Cryogenics	COBE, SHOOT
	Image Analysis Software	HEIDI, Yohkoh, & OVRO
	Solar Data Distribution	SMM, CGRO, Yohkoh & SOHO
PSI	Imager Tube, Grid Trays, and RAS and SAS	XMM RGS, SRG-EUVITA, & MIR-REM
Spectrum	Spacecraft and Mission I&T support	MSTI-1,-2,-3 MightySat, & New Millenium, DS-1

Figure G-2 Schedule

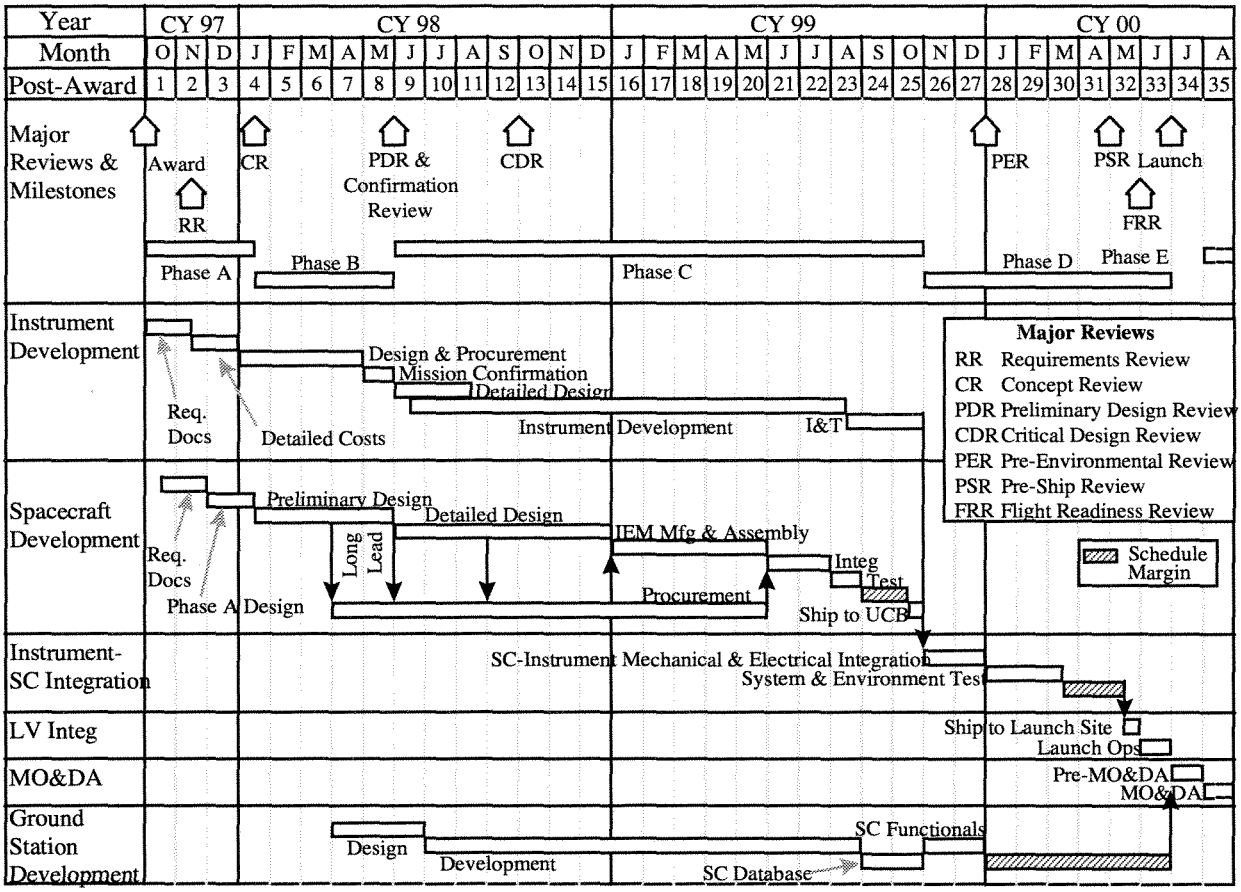

to provide straightforward, easily manageable interfaces between the team partners. GSFC tests, characterizes, and qualifies the grids and cryocooler, and delivers them to PSI and UCB, respectively. PSI fabricates the telescope, RAS, and SAS, and integrates them with the grids for the complete Imaging System. UCB fabricates the GeDs, cryostat, and instrument electronics, and integrates them with the cryocooler for the complete Spectrometer. These are integrated into the spacecraft fabricated by Spectrum Astro (under contract from UCB), and tested at UCB.

Mission and Science Operations are done at UCB. Data archiving and distribution is done by GSFC for U.S. researchers, and by ETH/Zurich for Europeans

G.2. Schedule

The top-level mission schedule (Fig. G-2) has a 3-month Concept Phase, a 23-month design and development phase, and 7 months for Mission I&T plus launch site operations. Included are 14 to 16 weeks of distributed slack for instrument and spacecraft, respectively. The instrument schedule of 20 months after concept phase to the start of instrument I&T is achievable with the simplifications itemized in Table H-1. **The design has no new technology items, 60% fewer detectors (12 GeDs + 12 SiDs to 9 GeDs), half the electronics, and requires minimal engineering.**

The pacing items in the instrument schedule were the cryocooler, the GeDs, and the grids. GSFC has agreed to supply the flight cryocooler immediately from their stock of qualified coolers, for the cost of replacing it. We have already performed GeD compatibility tests with the cooler. Grid characterization facilities are already in place at GSFC and, with fewer grids to fabricate and test, the Imaging System schedule has been improved. UCB technology for HESSI GeDs will be transferred to ORTEC Inc. to speed the fabrication of GeDs. By using the already developed and available spacecraft CPU and memory for instrument functions, instrument flight software development can start immediately.

The spacecraft schedule is based on previous efforts at Spectrum Astro, and is consistent with the design's maturity.

The ground system schedule is based on FAST. In parallel, the LEO-T ground station will be procured, installed at UCB and tested.

The spacecraft will be tested with the ground system at UCB while the instrument is in test/qual. This provides training time for the Flight Operations Team prior to MSI&T period.

H. COST

The HESSI team has been refining this mission concept for several years and fully understands the requirements, design implications and cost of the investigation. After HESSI's selection as an alternate in the MIDEX program, the NASA Office of Space Science challenged the HESSI team to develop a mission at SMEX cost able to meet the HESSI/MIDEX minimum science goals. The team together with the GSFC SMEX office produced the **HESSI-*Lite*** mission, which was presented to the Associate Administrator in January 1997, but was not started because of launch vehicle problems and other pressures on the budget.

The HESSI-*Lite* design is the basis for this HESSI/SMEX mission. Table H-1 lists the simplifications. All new technology development items, such as LIGA grids, have been deleted. Recent improvements in GeD performance from developments at UCB allowed us to delete the Si detectors. GSFC's cryogenics group has flight-qualified an inexpensive cryocooler, and UCB has proven its compatibility with GeDs.

Table H-1 HESSI-SMEX Simplifications

SubSystem	SMEX Modification
Si Detectors	**Deleted** entire subsystem (HV, CSA's, A/D circuitry)
Ge Detectors	**Reduced** qty (12 to 9)
Cryocooler	Selected SunPower cooler
LIGA Grids	**Deleted**
Stacked Grids	**Reduced** qty (9 to 7) Identical Front & Rear
CPU	**Deleted.** Using S/C CPU.
Memory	**Deleted.** Using S/C Mem
Propulsion	**Deleted.** Not needed for 38° orbit

The number of RMCs and GeDs is reduced from 12 to 9, and identical grids are now possible for the front and rear trays. With the 12 SiDs eliminated, the cryostat is simpler, and together with a more capable cryocooler and less heat load, the GeDs can be maintained much colder, enough to survive the radiation dose of an inclined orbit. Thus, the costly equatorial launch, the on-orbit propulsion system, the equatorial ground station, and communications costs, have been eliminated.

The spacecraft is built from already designed and qualified subsystems. Finally, the schedule is trimmed to reflect a greatly simplified system, now composed of mainly heritage designs.

Instrument. This category includes costs for management, science support, systems engineering, instrument systems, and instrument integration. The fabrication costs are based on FAST and Polar, with separately itemized GeD and grid cost based on the HIREGS and HEIDI programs.

Spacecraft. The spacecraft provider, Spectrum Astro, estimated the effort using a grass-roots method, itemizing the known cost of each qualified subsystem and its manpower. During the selection process, the cost for the spacecraft concepts received from the four industry finalists fell between $8 and $12M.

MSI&T costs are based on the FAST program, assuming a comparable effort for HESSI. Included are spacecraft and launch vehicle integration costs for Spectrum Astro.

Operations Preps costs are grass-roots estimates based on FAST. Costs of writing and testing data display and analysis software was estimated on the SDAC experience at handling similar requirements for SMM, Yohkoh, BATSE, and SOHO. Included also are **$300K for ground-based observatory upgrades.**

The **Ground Data System** cost is based upon the FUSE LEO-T cost, the GSFC cost for the ITOS system used for FAST, and actual costs of FAST database creation and CD production equipment.

The **MO&DA** costs are based on a grass-roots estimate, based on known FAST, Yohkoh, and Wind costs, assuming a 2-year operations lifetime and 3 years of data analysis. They include science operations, data analysis and distribution, maintenance for the LEO-T, and **$500K to fund a US Guest Investigator program**.

Budget Reserve. The budget contains a **development reserve of 20% on all components of the program**, except launch and MO&DA. This is more than ample, given the maturity of these efforts.

TABLE B1

TOTAL MISSION COST FUNDING PROFILE

(FY costs in Real Year Dollars, Totals in Real Year and FY 1997 Dollars) ($M)

Item	FY98	FY99	FY00	FY01	FY02	FY03	Total (Real Yr.)	Total (FY 1997)
Phase A	$ 0.259	$	$	$	$	$	$ 0.259	$ 0.250
Phase B/C/D	$ 15.520	$ 12.850	$ 9.541	$	$	$	$ 37.911	$ 35.425
Instrument	8.484	7.603	4.765				20.852	19.500
Spacecraft	6.868	4.255	0.563				11.686	11.075
MSI&T	0.168	0.992	4.213				5.373	4.850
Ground Data System Dev	$ 2.490	$ 0.643	$	$	$	$	$ 3.133	$ 3.000
Launch Services	$	$ 12.000	$ 7.000	$ 2.000	$	$	$ 21.000	$ 19.000
Phase E	$	$	$ 0.705	$ 3.418	$ 3.513	$ 3.133	$ 10.769	$ 9.000
Other (specify)	$	$	$	$	$	$	$	$
NASA Mission Cost	$ 18.269	$ 25.493	$ 17.246	$ 5.418	$ 3.513	$ 3.133	$ 73.072	$ 66.675
Contributions by Organization (Non-U.S. or U.S.) to:								
Phase A/B/C/D	$ 1.204	$ 0.865	$ 0.308	$	$	$	$ 2.377	$ 2.240
P. Scherrer Inst.	1.100	0.757	0.196				2.053	1.940
ETHZ	0.104	0.108	0.112				0.324	0.300
Ground Data System Dev	$	$	$	$	$	$	$	$
Launch Services	$	$	$	$	$	$	$	$
Phase E	$	$	$ 0.241	$ 1.317	$ 1.366	$ 1.027	$ 3.951	$ 3.305
NOAA			0.006	0.029	0.030	0.025	0.090	0.075
P. Scherrer Inst.			0.056	0.232	0.241	0.063	0.592	0.500
ETHZ			0.056	0.348	0.361	0.313	1.078	0.900
NAOJ			0.011	0.070	0.072	0.063	0.216	0.180
U. of Glasgow			0.056	0.348	0.361	0.313	1.078	0.900
Meudon			0.056	0.290	0.301	0.250	0.897	0.750
Other (specify)	$	$	$	$	$	$	$	$
Contributed Costs (Total)	$ 1.204	$ 0.865	$ 0.549	$ 1.317	$ 1.366	$ 1.027	$ 6.328	$ 5.545
				Mission Totals			$ 79.400	$ 72.220

Appendix I-4. References

Alexander, D. and Metcalf, T. 1997, submitted to *ApJ*.
Aschwanden, M. et al. 1996a, *ApJ*, **470**, 1198.
Aschwanden, M. et al. 1996b, *ApJ*, **468**, 398.
Aschwanden, M. et al. 1996c, *ApJ*, **464**, 974.
Bahcall, J. N., and Pinsonneault, M. H. 1995, *Rev. Mod. Phys.* **67**, 781.
Band, D.L. et al. 1994 *ApJ* **434**, 560.
Benka, S.G., and Holman, G.D. 1994 *ApJ*, **435**, 469.
Bietenholz, M.F. & Kronberg, P.P. 1992, *ApJ*, **393**, 206.
Canfield, R.C. et al. 1993 *ApJ* **411**, 362.
Chupp, E.L. 1990 *Physica Scripta*, **T18**, 15.
Cliver, E. et al. 1986, *ApJ* **305**, 920.
Crannell, C.J. et al. 1976 *ApJ* **210**, 52.
Dennis, B.R., and Zarro, D.M., 1993 *Solar Phys.*, **146**, 177.
Emslie, G. et al. 1997, *ApJ (in press)* **485.**
Feffer, P.T. et al. 1993, *Astron. Astrophy. Suppl.*, **97**, 31.
Fishman, G. et al., 1994, *Science*, **264**, 1313.
Gopalswamy, N. and Kundu, M.R., 1995, *ApJ*, 223.
Gopalswamy, N. et al. 1997, *ApJ*, **475**, 348.
Harmon, B. A. et al. 1992, in *Proc. of the CGRO Workshop*, p. 69.
Henoux , J.C. et al. 1990 *ApJ Suppl.* **73**, 303.
Hernandez, B.P. and Christensen-Dalsgaard, J. 1994, *MNRAS*, **269**, 474.
Holman, G.D., 1995 *ApJ*, 452, 451.
Horack, J.M. et al. 1992, *1992 Huntsville Gamma-Ray Burst Workshop*, 373.
Hua, X.M. & Lingenfelter, R.E. 1987, *Solar Phys.* **113**, 229.
Hua, X. M. et al. 1989 *ApJ* **341**, 516.
Hudson, H.S. et al. 1994, in *X-ray Solar Physics from Yohkoh, UAP, Tokyo*, p. 143.
Hudson, H.S.1978, *ApJ* **224**, 235.
Johns,C. and Lin, R.P. 1992, *Solar Phys.* **137**, 121.
Kahler, S.W., 1992, *Annual Review of Astronomy and Astrophysics*, **30**, 113.
Kanbach, G. et al. 1993 *A&A Suppl.* **97**, 349.
Kane, S.R. et al. 1992 *ApJ* **390**, 687.
Kiplinger, A.L., 1995, *ApJ,* **453**, 973.
Kundu, M.R. et al. 1995 *ApJ* **444**, 922.
Kundu, M.R. et al. 1990, *ApJ*, **358**, L69.
Kurt, V. et al. 1996, in *High Energy Solar Physics, AIP*, p. 237.
Ramaty, R. et al. *ApJ*, **455**, L193, 1995.
Landis, D.A. et al., 1982, *IEEE Trans. Nuc. Sci.* **NS-29**, 619, 1982.
Lin, R.P., 1990, in *Basic Plasma Processes on the Sun*, p. 467
Lin, R.P., 1997, *AIP Conf. Proc.* **385**, 25.
Lin, R.P., and Hudson, H.S., *Solar Phys.* **50**, 153, 1976.
Lin, R.P., and Johns, C., 1993, *ApJ Letters* **417**, L53.
Lin, R.P. and Schwartz, R.E. 1987, *ApJ* **312**, 462.
Lin, R.P. et al. 1981 *ApJ Letters* **251**, 109.
Lin, R.P. et al. 1984, *ApJ* **283**, 421.
Lin, R.P. et al. 1996, *GRL* **23**, 1211.
Luke, P.N., 1984, *IEEE Trans. Nucl. Sci*, **N5-31**, 312.
Mandzhavidze, N. et. al., 1997, *Proc, 25th ICRC*, in press.
Masudas, S. et al. *Nature*, **371**, 495, 1994.
Metcalf , T.R. et al. 1993, *AIP Conf. Proc.* **294**, 59.
Miller, J.A. et al. 1997, *JGR (in press).*
Nishio, M. 1997, *ApJ (in press).*
Parker, E.N. 1988, *ApJ* **330**, 474.
Pelling, R.M. et al. 1987, *ApJ* **319**, 416.
Pelling R.M. et al. 1992. In *Proc. SPIE Meeting*, San Diego, July 1992.
Prince, T.A. et al. 1988 *Solar Phys.* **118**, 269.
Ramaty, R., and Murphy, R.J., 1987, *Sp. Sci Rev.* **45**, 213.
Ramaty, R. et al. 1993, *Adv. Space Res.* **13**, 275, 1993.
Ramaty, R. et al. 1995, *Astrophys. J. Lett.*, in press.
Rank, G., 1996, in *High Energy Solar Physics*, AIP, p. 402
Reames, D.V. 1994 *ApJ Suppl.* **73**, 235.
Reames, D.V. 1996, *AIP Conf. Proc.*, no. 374, 35.
Reames, D.V. et al. 1994 *ApJ Suppl.* **90**, 649.
Reames, D.V. et al. 1985 *ApJ* **292**, 716.
Sakao, T. et al. 1994 *Kofu Symp.*, NRO report No. **360**, 169.
Share, G.H. and Murphy, R.J. 1995, *ApJ*, **452**, 933.
Share, G.H., and Murphy, R.J., 1997, *ApJ*, in press.
Shibata K. et al. 1992 *PASJ* **44**, L173.
Shimizu, T., *Publ. Astron. Soc. Japan*, **47**, 251, 1995.
Smith, D.M. et al. 1993, *Astrophys. J.* **414**, 165.
Smith, D.M. et al. 1995, *J. Geophys.* Res. **100,** 19675.
Temerin and Roth 1991, *Astrophys. J.* 391, L.105.
Thompson, B. et al. 1997, in preparation.
van Beek et al. 1980, *Solar Phys.* **65**, 39.
Vestrand, W.T. and Forrest, D.J., 1993, *ApJ, Letters*, **409**, 69.
Wagner and McQueen, 1983, *Astron. Astrophys.* **120**, 136.
Wülser, J. –P. et al. 1995, *Astron. Astrophys.*, submitted.
Zhang, S. N. et al. 1993, *Nature* **366**, 245.

Appendix I-4. Acronyms

ACE	Advanced Composition Explorer
ACS	Attitude Control System
ADC	Analog-to-Digital Converter
AO	Announcement of Opportunity
AU	Astronomical Unit
BATSE	Burst and Transient Source Experiment on CGRO
BBSO	Big Bear Solar Observatory, operated by Caltech
BER	Bit Error Rate
BIMA	Berkeley-Illinois-Maryland Array, a radio interferometer in CA
BPSK	Binary Phase Shift Keying
CCB	Charge Control Board
CCD	Charge Coupled Device
CCSDS	Consultative Committee for Space Data Systems
CDR	Critical Design Review
CDS	Coronal Diagnostic Spectrometer (on SOHO)
CEA	Center for EUV Astrophysics
CG	Center of Gravity
C&DH	Command and Data Handling
CD-ROM	Compact Disk - Read Only Memory
CGRO	Compton Gamma Ray Observatory
CIB	Communications Interface Board
CM	Configuration Management
CME	Coronal Mass Ejection
COBE	Cosmic Background Explorer
CoI	Co-investigator
CPU	Central Processor Unit
CPV	Common Pressure Vessel
CR	Concept Review
CSA	Charge-Sensitive Amplifier
CsI	Cesium Iodide scintillator
Cu	Copper
DC	Direct Current
DC-DC	Direct Current to Direct Current Converter
$\Delta E/E$	Fractional energy resolution
DISCR	Discriminator
DMA	Direct Memory Access
D/NAR	Design/Non-Advocate Review
DS-1	Deep Space 1 spacecraft
e/p	Electron-to-proton ratio
EFI	Electric Field Instrument for Polar spacecraft
EGRET	Energetic Gamma Ray Experiment on CGRO
EIT	Extreme Ultraviolet Telescope (on SOHO)
ELV	Expendable Launch Vehicle
EPO	Education & Public Outreach
ESA	European Space Agency
ESD	ElectroStatic Discharge
ETH	Eidgen"ossische Technische Hochschule in Zurich, Switzerland
ETU	Engineering Test Unit
EUV	Extreme Ultra Violet
EUVE	Extreme Ultra-Violet Explorer
EUVITA	Extreme Ultraviolet Imaging Telescope Array on SRG
FAST	Fast Auroral SnapshoT Explorer, a SMEX mission
FET	Field Effect Transistor
FIP	First Ionization Potential
FITS	Flexible Image Transport System, a standard file specification
FMEA	Failure Modes and Effects Analysis
FOV	Field of View
FUSE	Far Ultraviolet Spectroscopic Explorer
FWHM	Full-Width at Half-Maximum
FY	Fiscal Year
Gbits	Giga bits (10^9 bits)
Gbytes	Giga bytes (10^9 bytes)
GCF	Grid Characterization Facility
Ge	Germanium
GeD	Germanium Detector
GEANT	A Monte Carlo code for modeling X-ray/Gamma-ray detectors
GeV	Giga (10^9) electron Volts
GEVS	General Environmental Verification Specification (GSFC)
GOES	NOAA's Geostationary Operational Environmental Satellite
Grms	Root mean square acceleration level in units of Earth gravity
GRS	Gamma-Ray Spectrometer on SMM
GSFC	Goddard Space Flight Center
Hα	Optical emission line from atomic hydrogen
HEAO-3	High Energy Astrophysics Observatory-3
HEDC	High Energy Data Center
HEIDI	High Energy Imaging Device, a GSFC balloon payload
HESI	High Energy Solar Imager, a NASA study that followed HESP
HESP	High Energy Solar Physics mission, a NASA study that preceded HESI
HESSI	High Energy Solar Spectroscopic Imager

HEXAGONE	High Energy X-ray and Gamma-ray Observatory for Nuclear Emissions, a UCB balloon instrument
HIREGS	High Resolution Gamma Ray Spectrometer, a UCB balloon instrument
HIREX	High Resolution X-ray Spectrometer, a UCB balloon instrument
HVPS	High Voltage Power Supply
HXIS	Hard X-ray Imaging Spectrometer on SMM
HXRBS	Hard X-ray Burst Spectrometer on SMM, a GSFC instrument
HXT	Hard X-ray Telescope on Yohkoh
Hz	Hertz (cycles per second)
I&T	Integration and Test
IDL	Interactive Data Language from Research Systems, Inc.
IDPU	Instrument Data Processing Unit
IEM	Integrated Electronics Module
INTEGRAL	ESA's International Gamma-Ray Astrophysics Laboratory
IPM	Instrument Project Manager
IR	Infra-Red
ITOS	Integrated Test and Operations System
JPL	Jet Propulsion Laboratory
kbps	kilo-bits per second
keV	kilo (10^3) electron Volts
KP	Kitt Peak National Observatory
K through 12 (or K-12)	Kindergarten through 12^{th} grade
L	Distance between grids in an RMC
LASCO	Large Angle Spectroscopic Coronagraph (on SOHO)
LEO-T	Low Earth Orbit Tracking station
LIGA	Lithografie, Galvanoformung, Abformtechnik (German name for deep-etch X-ray lithography of acrylic resists, electroforming, and replication)
LLD	Lower-Level Discriminator
LN_2	Liquid Nitrogen
LO-AX	Trademark for low energy germanium detector made by ORTEC
LSB	Least-Significant Bit
LSEP	Large Solar Energetic Potential
LV	Launch Vehicle
Max '91	A joint NASA/NSF program during the 1991 solar maximum.
M-B	Molecular Beam
Mbits	Mega bits (10^6 bits)
MDI	Michelson Doppler Imager (on SOHO)
MeV	Mega (10^6) electron Volts
MIDEX	Mid-sized Explorer
MIR	A Russian satellite
MightySat	USAF Philips Lab Spacecraft
MLI	Multi-Layer Insulation
MO&DA	Mission Operations and Data Analysis
MOC	Mission Operations Center
MSI&T	Mission-Specific Integration & Test
MSTI	Miniature Sensor Technology Integration satellites
MSU	Montana State University
NA or N/A	Not Applicable
NaI	Sodium Iodide (scintillator)
NAOJ	National Astronomical Observatory of Japan
NAR	Non-Advocacy Review
NASA	National Aeronautics and Space Administration
NASTRAN	NASA Structural Analysis program
^{20}Ne	Neon isotope
NHB	NASA Handbook
NMP	New Millenium Program
Ni	Nickel
NiCd, Ni-Cad	Nickel Cadmium
NOAA	National Oceanic and Atmospheric Administration
NORAD	NORth American Defense Command
NSF	National Science Foundation
NSO	National Solar Observatory in Tucson, AZ
NSSDC	National Space Science Data Center
OGCF	Optical Grid Characterization Facility
OLS	Orbital Launch Services Project at GSFC
ORTEC	a nuclear instrumentation company
OSSE	Oriented Scintillation Spectrometer Experiment on CGRO
OVRO	Owens Valley Radio Observatory operated by Caltech
p	pitch of a grid
PA	Performance Assurance
PACI	Payload and Altitude Control Interface
Pb	Lead
PC	Personal Computer
Pegasus XL	Launch vehicle built by Orbital Science Corporation
PI	Principal Investigator
PIO	Power Input/Output
PPL	Preferred Parts List
RAM	Random Access Memory
RAS	Roll Angle System
REM	Radiation Environment Monitor, on MIR
REU	Research Experiences for Undergraduates, an NSF Outreach Program

RF	Radio Frequency
RMC	Rotating Modulation Collimator
ROSAT	Roentgen Satellite, a German X-ray telescope
RPM	Revolutions Per Minute
RR	Requirements Review
RSTN	Radio Solar Telescope Network - USAF
RS232	IEEE interface specification for serial data transfer
S/A	Solar Array
S&E	Supplies & Expenses
SAA	South Atlantic Anomaly
SAMPEX	Solar, Anomalous, and Magnetospheric Particle Explorer
SAS	Solar Aspect System on HESSI
SB	Small Business
SBIR	Small Business Innovative Research
S/C	Spacecraft
SDAC	Solar Data Analysis Center at GSFC
SDB	Small Disadvantaged Business
SEGway	Science Education Gateway project (UC Berkeley)
SEC	NOAA Space Environment Center
SELVS II	Small Expendable Launch Vehicle Services II
SEP	Solar Energetic Particle
SHOOT	Superfluid Helium On-Orbit Transfer experiment
Si	Silicon
SiD	Silicon Detector
SINDA	Systems Improved Differencing Analyzer (thermal analysis software)
SMA	Shape Memory Alloy
SMEX	Small Explorer
SMM	Solar Maximum Mission (1980-1989)
Sn	Tin
SOC	Science Operations Center
SOHO	Solar and Heliospheric Observatory
SOON	USAF's Solar Optical Observing Network
SP	NSO's Sacramento Peak Observatory
SPRC	Space Physics Research Center
S/R	Shift Register
SRG	Spectrum Roentgen Gamma
SR&T	Supporting Research and Technology
SSL	Space Sciences Laboratory at UCB
SSR	Solid-State Recorder
STDN	Space Tracking Data Network
SUMER	Solar Ultraviolet Measurement of Emitted Radiation on SOHO
SWRI	Southwest Research Institute
SXI	Soft X-ray Imager on GOES
SXT	Soft X-ray Telescope on Yohkoh
t	Thickness of a grid
TBD	To Be Determined
TDU	Telescope Demonstration Unit
TGRS	Transient Gamma-Ray Spectrometer on Wind
TM or T/M	Telemetry
TMS	Twist Monitoring System
TRACE	Transition Region And Corona Explorer
T/V	Thermal Vacuum
UAH	University of Alabama at Huntsville
UC	University of California
UCB	University of California, Berkeley
ULD	Upper-Level Discriminator
Ulysses	"Solar Polar" Mission
US	United States
USAF	United States Air Force
UV	Ultraviolet
VLA	Very Large Array, radio interferometer at Socorro, NM
VME	Virtual Memory Extended
w	Grid slit width
W	Watt or the element tungsten
WBS	Work Breakdown Structure
Wind	An ISTP spacecraft to study the solar wind
WWW	World Wide Web
XDL	Cross Delay Line detector in the Summer instrument on SOHO
XMM	X-ray Multi-Mirror Mission
XTE	X-ray Timing Explorer
Yohkoh	Japanese solar spacecraft launched in 1991
Z	Atomic number or axis in a Cartesian coordinate system
3DP	Three-Dimensional Plasma instrument on Wind spacecraft